Journal of Cardiovascular Pharmacology

Dexmedetomidine exerts a negative chronotropic action on sinoatrial node cells through the activation of imidazoline receptors

--Manuscript Draft--

Manuscript Number:	JCVP-21-273R1
Full Title:	Dexmedetomidine exerts a negative chronotropic action on sinoatrial node cells through the activation of imidazoline receptors
Article Type:	Original Article
Section/Category:	CARDIAC
Keywords:	dexmedetomidine, α2-adrenoceptor, imidazoline receptor, sinoatrial node cells, hyperpolarization-activated cation current, automaticity
Corresponding Author:	Wei-Guang Ding, Ph.D. Shiga University of Medical Science: Shiga Ika Daigaku Otsu, Shiga JAPAN
Corresponding Author Secondary Information:	
Corresponding Author's Institution:	Shiga University of Medical Science: Shiga Ika Daigaku
Corresponding Author's Secondary Institution:	
First Author:	Mariko Ishihara, M.D.
First Author Secondary Information:	
Order of Authors:	Mariko Ishihara, M.D.
	Akiko Kojima, M.D., Ph.D.
	Wei-Guang Ding, M.D., Ph.D.
	Hirotoshi Kitagawa, M.D., Ph.D.
	Hiroshi Matsuura, M.D., Ph.D.
Order of Authors Secondary Information:	
Manuscript Region of Origin:	JAPAN
Abstract:	Dexmedetomidine (DEX), an α2-adrenoceptor (α2-AR) and imidazoline receptor (IR) agonist is most often used for the sedation of patients in the intensive care unit. Its administration is associated with an increased incidence of bradycardia; however, the precise mechanism of DEX-induced bradycardia has yet to be fully elucidated. The present study was undertaken to examine whether DEX modifies pacemaker activity and the underlying ionic channel function through α2-AR and IR receptors. The whole-cell patch-clamp techniques were used to record action potentials and related ionic currents of sinoatrial (SA) node cells in guinea pigs. DEX (≥10 nM) reduced SA node automaticity and the diastolic depolarization rate. DEX reduced the amplitude of hyperpolarization-activated cation current (If, Ih) the pacemaker current, even within the physiological pacemaker potential range. DEX slowed the If current activation kinetics and caused a significant shift in the voltage-dependence of channel activation to negative potentials. In addition, efaroxan, an α2-AR and imidazoline I1 receptor (I1R) antagonist, attenuated the inhibitory effects of DEX on SA node automaticity and If current activity, while yohimbine, an α2-AR selective antagonist, did not. DEX did not affect the current activities of other channels, including rapidly and slowly activating delayed rectifier K+ currents (IKr and IKs), L-type Ca2+ current (ICa,L), Na+/Ca2+ exchange current (INCX), and muscarinic K+ current (IK,ACh). Our results indicate that DEX, at clinically relevant concentrations, induced a negative chronotropic effect on the SA node function through the downregulation of If current via an I1R other than the α2-AR in the clinical setting.
Suggested Reviewers:	

Abstract:

Dexmedetomidine (DEX), an α_2-adrenoceptor (α_2-AR) and imidazoline receptor (IR) agonist is most often used for the sedation of patients in the intensive care unit. Its administration is associated with an increased incidence of bradycardia; however, the precise mechanism of DEX-induced bradycardia has yet to be fully elucidated. The present study was undertaken to examine whether DEX modifies pacemaker activity and the underlying ionic channel function through α_2-AR and IR receptors. The whole-cell patch-clamp techniques were used to record action potentials and related ionic currents of sinoatrial (SA) node cells in guinea pigs. DEX (≥10 nM) reduced SA node automaticity and the diastolic depolarization rate. DEX reduced the amplitude of hyperpolarization-activated cation current (I_f, I_h) the pacemaker current, even within the physiological pacemaker potential range. DEX slowed the I_f current activation kinetics and caused a significant shift in the voltage-dependence of channel activation to negative potentials. In addition, efaroxan, an α_2-AR and imidazoline I_1 receptor (I_1R) antagonist, attenuated the inhibitory effects of DEX on SA node automaticity and I_f current activity, while yohimbine, an α_2-AR selective antagonist, did not. DEX did not

affect the current activities of other channels, including rapidly and slowly activating delayed rectifier K^+ currents (I_{Kr} and I_{Ks}), L-type Ca^{2+} current ($I_{Ca,L}$), Na^+/Ca^{2+} exchange current (I_{NCX}), and muscarinic K^+ current ($I_{K,ACh}$). Our results indicate that DEX, at clinically relevant concentrations, induced a negative chronotropic effect on the SA node function through the downregulation of I_f current via an I_1R other than the α_2-AR in the clinical setting.

Dexmedetomidine exerts a negative chronotropic action on sinoatrial node cells through the activation of imidazoline receptors

Mariko Ishihara, M.D.[1,2], Akiko Kojima, M.D., Ph.D.[2], Wei-Guang Ding, M.D., Ph.D.[1], Hirotoshi Kitagawa, M.D., Ph.D.[2], Hiroshi Matsuura, M.D., Ph.D.[1]

[1] Department of Physiology, Shiga University of Medical Science, Otsu, Shiga, 520-2192, Japan

[2] Department of Anesthesiology, Shiga University of Medical Science, Otsu, Shiga, 520-2192, Japan

Name and address for correspondence:

Wei-Guang Ding, MD, PhD,

Department of Physiology

Shiga University of Medical Science

Seta Tsukinowa-cho, Otsu, Shiga, 520-2192, Japan

Phone: +81 77 548 2152

Fax: +81 77 548 2348

E-mail: ding@belle.shiga-med.ac.jp

A short running title: DEX inhibits SA node automaticity via I_1R

Declaration of Finding Source: This study was supported by JSPS (The Japan Society for the Promotion of Science, Tokyo, Japan) KAKENHI Grant Numbers 17K11050 (to Akiko Kojima) and 17K08536 (to Hiroshi Matsuura).

Conflict of Interest Disclosure: The authors declare no conflicts of interest in association with the present study.

Abstract:

Dexmedetomidine (DEX), an α_2-adrenoceptor (α_2-AR) and imidazoline receptor (IR) agonist is most often used for the sedation of patients in the intensive care unit. Its administration is associated with an increased incidence of bradycardia; however, the precise mechanism of DEX-induced bradycardia has yet to be fully elucidated. The present study was undertaken to examine whether DEX modifies pacemaker activity and the underlying ionic channel function through α_2-AR and IR receptors. The whole-cell patch-clamp techniques were used to record action potentials and related ionic currents of sinoatrial (SA) node cells in guinea pigs. DEX (≥10 nM) reduced SA node automaticity and the diastolic depolarization rate. DEX reduced the amplitude of hyperpolarization-activated cation current (I_f, I_h) the pacemaker current, even within the physiological pacemaker potential range. DEX slowed the I_f current activation kinetics and caused a significant shift in the voltage-dependence of channel activation to negative potentials. In addition, efaroxan, an α_2-AR and imidazoline I_1 receptor (I_1R) antagonist, attenuated the inhibitory effects of DEX on SA node automaticity and I_f current activity, while yohimbine, an α_2-AR selective antagonist, did not. DEX did not affect the current activities of other channels, including rapidly and slowly activating delayed rectifier K^+ currents (I_{Kr} and I_{Ks}), L-type Ca^{2+} current ($I_{Ca,L}$), Na^+/Ca^{2+} exchange current

(I_{NCX}), and muscarinic K^+ current ($I_{K,ACh}$). Our results indicate that DEX, at clinically relevant concentrations, induced a negative chronotropic effect on the SA node function through the downregulation of I_f current via an I_1R other than the α_2-AR in the clinical setting.

Key words: dexmedetomidine, α_2-adrenoceptor, imidazoline receptor, sinoatrial node cells, hyperpolarization-activated cation current, automaticity

Data availability statement

The data that support the findings of this study are available from the corresponding author upon reasonable request.

Acknowledgment

The authors are grateful to Orion Corporation (P.O. Box 65, FI-02101 Espoo, Finland) for the generous gift of dexmedetomidine.

Introduction

Dexmedetomidine (DEX), a selective α_2-adrenoreceptor (α_2-AR) agonist, is most often used for the sedation of mechanically ventilated patients in the intensive care unit (ICU) as well as for non-intubated patients receiving local anesthesia for various surgical operations and procedures, because it is not associated with respiratory depression.[1] On the other hand, a number of studies have demonstrated that DEX has various cardiovascular side effects, including hypotension, hypertension and bradycardia.[2-4] For example, the perioperative use of DEX for congenital heart surgery evokes bradyarrhythmias[5] and in another meta-analysis, the perioperative use of DEX in patients undergoing cardiac surgery was reported to increase the risk of bradycardia and reduce the risk of tachycardia.[6] In addition, some case reports have shown that DEX produces severe bradycardia and even asystole.[7-9] In the clinical setting, it is recommended that DEX be administered at a dose of 1 μg/kg over 10 min for initial loading, followed by infusion at 0.2-07 μg/kg/h. The plasma concentration of DEX can reach approximately 10 nM after an initial loading dose.[10] However, both the loading dose and a high maintenance dose of DEX were demonstrated to increase the risk of bradycardia in patients[4] and to cause a significant reduction in the heart rate of healthy volunteers.[2]

The following mechanisms are considered to cause DEX-induced bradycardia: i) in the

nucleus tractus solitarii, stimulation of α_2-AR results in hypotension and bradycardia by facilitating the baroreceptor reflex[11]; ii) stimulation of α_2-AR in the rostral ventrolateral medulla (RVLM) neurons reduces sympathetic nerve activity, leading to a reduction in the release of adrenaline and noradrenaline[12,13]; iii) α_{2A}-adrenoreceptors suppress the release of noradrenaline by presynaptic feedback at the sympathetic nerve terminal[14]; iv) stimulation of α_{2C}-adrenoreceptors in the adrenal medulla decreases the secretion of adrenaline through the inhibition of voltage-gated Ca^{2+} channel activity[14]; and v) in the blood vessels, stimulation of α_{2B}-adrenoreceptors induces vasoconstriction, which is followed by an increase in blood pressure and slowing of the heart rate via the baroreceptor reflex.[2,14]

Based on these anatomical and physiological observations, it is reasonable to assume that DEX primarily induces bradycardia through neurohumoral mechanisms. A clinical electrophysiological study reported that DEX decreases the heart rate and prolongs the PR interval in children by depressing the sinoatrial (SA) and atrioventricular nodal functions mediated through a reduction in sympathetic nerve activity.[15] On the other hand, a study using an microelectrode method demonstrated that DEX decreased the firing rate in rabbit SA node tissue.[16] Thus, the negative chronotropic effect of DEX appears to arise from its direct and/or indirect effects on SA node cells. Interestingly, some α_2-AR agonists, such as DEX

and clonidine, possess an imidazoline structure,[13] and can thereby functionally bind to and stimulate the imidazoline receptor (IR).[17] However, it remains unknown whether or not DEX directly inhibits the SA node function through either α_2-AR or IR signaling pathway.

The present study was undertaken to investigate the direct effects of DEX on SA node cell automaticity and its underlying ionic mechanisms and to examine whether both α_2-AR and IR contribute to the direct effect of DEX on pacemaker activity.

Methods

Preparation of SA node cells

This investigation complied with the Guide for the Care and Use of Laboratory Animals published by the United States National Institutes of Health (NIH publication No. 85-23, revised 1996), and all experimental protocols were approved by the Institutional Animal Care and Use Committee of Shiga University of Medical Science (approval number, 2017-2-4H1). Single SA node cells were isolated from 5–8- week-old female Hartley guinea pigs (250–400 g) that were deeply anesthetized with an overdose of sodium pentobarbital (120 mg/kg), using a previously described enzymatic dissociation procedure.[18-20] In short, the guinea pig heart was excised and retrogradely perfused using a Langendorff apparatus at 37 °C, initially for 4 min with normal Tyrode solution containing (in mM) 140 NaCl, 5.4 KCl, 1.8 $CaCl_2$, 0.5 $MgCl_2$, 0.33 NaH_2PO_4, 5.5 glucose and 5 HEPES (PH adjusted to 7.4 with NaOH) and then for 4 min with Ca^{2+}-free Tyrode solution and for 10 min with Ca^{2+}-free Tyrode solution containing collagenase (0.04%) (Wako Pure Chemical Industries, Osaka, Japan). The SA node region bordered by the superior vena cava, the crista terminalis and the intra-atrial septum was cut out from the heart. The SA node tissue was further digested for 24 min via incubation at 37 °C with Ca^{2+}-free Tyrode solution containing collagenase (0.1%) and

elastase (0.01%) (Wako Pure Chemical Industries). Finally, the SA node strips were gently agitated to release SA node cells. The cells were stored at 4 °C in the KB solution for experimental use within 8 h. The KB solution contained (in mM) 70 K-glutamate, 30 KCl, 10 KH_2PO_4, 1 $MgCl_2$, 20 taurine, 0.3 EGTA, 10 glucose and 10 HEPES (pH adjusted to 7.2 with KOH).

Whole-cell patch-clamp techniques

The perforated and conventional whole-cell patch-clamp techniques were used to record spontaneous action potentials and ionic currents in the current- and voltage-clamp models, respectively, at 36 ± 1°C with an EPC-8 patch-clamp amplifier (HEKA, Lambrecht, Germany). In the present study, the SA node cells were identified based on their morphological characteristics, such as spindle- and spider-shaped cells as previously reported.[21,22] In addition, these cells often usually generate spontaneous automaticity in normal Tyrode solution, whereas atrial-shaped myocytes demonstrate no spontaneous contraction. The spontaneous action potentials were recorded using a fire-polished patch pipette (resistance, 2.0–4.0 MΩ) filled with the pipette solution containing (in mM) 70 potassium aspartate, 50 KCl, 10 KH_2PO4, 1 $MgSO_4$, 3 ATP (disodium salt; Sigma Chemical

Company, St Louis, MO, USA), 5 EGTA, and 5 HEPES and 0.1 Li_2-GTP (Sigma Chemical Company) (pH adjusted to 7.2 with KOH). Amphotericin B (Wako Pure Chemical Industries) was added to the pipette solution at a concentration of 100 μg/ml. An aliquot of isolated cells was placed into a recording chamber (0.5 ml in volume) and was superfused at 35-37°C with normal Tyrode solution.[18-20] Dexmedetomidine hydrochloride (Orion Corporation, FI-02101 Espoo, Finland; Tokyo Chemical Industry, Japan) was dissolved in dimethyl sulfoxide, and then diluted in Tyrode solution to concentrations of 5 nM, 10 nM, 100 nM and 1 μM. In some experiments, the spontaneous action potentials were recorded in the presence of moxonidine (Tokyo Chemical Industry) or phorbol 12-myristate 13-acetate (PMA) (Sigma Chemical Company). In some experiments, after superfusion of Tyrode solution containing yohimbine (Sigma Chemical Company), efaroxan (Sigma Chemical Company), idazoxan (Sigma Chemical Company) or bisindolylmaleimide I (BIS-I) (Sigma Chemical Company) for approximately 4-5 min until reaching a steady state, the cells were exposed to DEX.

Hyperpolarization-activated cation current (I_f, I_h) was recorded in Tyrode solution supplemented with 2 mM $NiCl_2$ and 0.5 mM $BaCl_2$ to eliminate voltage-dependent Ca^{2+} current and Ba^{2+}-sensitive K^+ current, respectively, using K^+-rich pipette solution. The pipette solution contained (in mM) 70 potassium aspartate, 50 KCl, 10 KH_2PO4, 1 $MgSO_4$, 3 ATP

(disodium salt; Sigma Chemical Company), 5 EGTA, 5 HEPES, 2 $CaCl_2$ and 0.1 Li_2-GTP (pH adjusted to 7.2 with KOH). I_f was activated by 2-s hyperpolarizing voltage-clamp steps applied from a holding potential of -40 mV to test potentials of -50 mV to -140 mV.[19,20,23] I_f was measured as the difference between the instantaneous and the steady state current levels. The I_f conductance (g_f) at each test potential was calculated according to the following equation: $g_f = I_f / (V_t - V_{rev})$, where I_f is current density, V_t is test potential, and V_{rev} is the reversal potential for I_f. The voltage dependence of I_f activation was assessed by fitting g_f to a Boltzmann equation: $g_f = g_{f,max} / (1 + \exp((V_t - V_h) /k))$, where $g_{f,max}$ is the fitted maximal conductance of I_f, V_h is the voltage at half-maximal activation and k is the slope factor. The activation time course of I_f was evaluated by fitting currents at -140 mV to two exponential functions. In some experiments, I_f current was recorded in the presence of ivabradine (Tokyo Chemical Industry), moxonidine and rilmenidine (BLD Pharmatech, Shanghai, China).

The rapidly activating delayed rectifier K^+ current (I_{Kr}) was measured in Tyrode solution supplemented with HMR 1556 (Hoechst Marion Roussel, Frankfurt, Germany) and nisoldipine (Sigma Chemical Company) to eliminate the slowly activating delayed rectifier K^+ current (I_{Ks}) and the L-type Ca^{2+} current ($I_{Ca,L}$), respectively. I_{Kr} current was activated by 250-ms depolarizing steps applied from a holding potential of -50 mV to test potentials of -40

mV to +50 mV.[19,20] I_{Ks} current was recorded in the presence of E-4031, an I_{Kr} channel antagonist (Wako Pure Chemical Industries) and nisoldipine to eliminate I_{Kr} and $I_{Ca,L}$, respectively. I_{Ks} current was activated by 2-s depolarizing steps applied from a holding potential of -50 mV to test potentials of -40 mV to +50 mV.[18-20] The activation of I_{Kr} and I_{Ks} was evaluated by measuring the amplitude of tail currents elicited on repolarization to the holding potential. The voltage dependence of I_{Kr} and I_{Ks} activation was assessed by fitting the amplitude tail current (I_{tail}) to a Boltzmann equation: $I_{tail} = I_{tail,max} / (1 + \exp((V_h - V_t) /k))$, where $I_{tail,max}$ is the fitted maximal tail current density of I_{Kr} or I_{Ks}.

$I_{Ca,L}$ was measured in K^+- free Cs Tyrode solution containing (in mM) 140 NaCl, 5.4 CsCl, 1.8 $CaCl_2$, 0.5 $MgCl_2$, 5.5 glucose and 5 HEPES (PH adjusted to 7.4 with NaOH). The pipette solution was a Cs^+-rich solution containing (in mM) 90 cesium aspartate, 30 CsCl, 20 tetraethylammonium chloride, 2 $MgCl_2$, 5 ATP (Mg salt; Sigma Chemical Company), 5 phosphocreatine (disodium salt; Sigma Chemical Company), 0.1 Li_2-GTP (Sigma Chemical Company), 5 EGTA and 5 HEPES (PH adjusted to 7.2 with CsOH). Ca^{2+} current was recorded with 500-ms depolarizing steps applied from a holding potential of -50 mV to the test potential of -10 mV.[24,25] Two experimental protocols were applied. One was recording $I_{Ca,L}$ current for 15 min (a time-matched control); the other was recording for 15-20 min,

before and during exposure to DEX, respectively.

Na^+/Ca^{2+} exchange current (I_{NCX}) was recorded in K^+- free Cs Tyrode solution supplemented with ouabain (Sigma Chemical Company), ryanodine (Alomone labs, Ltd. Israel) and nisoldipine to inhibit Na^+/K^+ pump, ryanodine receptor and $I_{Ca,L}$, respectively. The pipette solution contained (in mM) 90 cesium aspartate, 20 CsCl, 20 tetraethylammonium chloride, 10 NaCl, 2 $MgCl_2$, 1.75 $CaCl_2$, 5 ATP (Mg salt; Sigma Chemical Company), 5 BAPTA and 10 HEPES (pH adjusted to 7.2 with CsOH). Membrane currents were measured at a holding potential of -40 mV, during the hyperpolarizing phase from +40 mV to -120 mV of the voltage-ramp protocol.[19] After recording the baseline current, DEX was exposed and followed by the administration of $NiCl_2$ to fully block I_{NCX} current. Muscarinic K^+ current ($I_{K,ACh}$) was measured in Tyrode solution supplemented with nisoldipine (0.4 μM), using K^+-rich pipette solution. Membrane currents were recorded at a holding potential of -40 mV, during the hyperpolarizing phase from +40 mV to -120 mV of the voltage-ramp protocol.[20] After recording the baseline current, the cell was exposed to DEX and then exposed to acetylcholine (ACh) to activate $I_{K,ACh}$ current.

Statistical analysis

The results are expressed as the mean ± SD, with the number of animals and experiments indicated by *N* and *n*, respectively. Error bars in the figures indicate the SD with *n* given in parentheses. The results were statistically analyzed by a one-way ANOVA followed by *Dunnett's* test, a paired *t* test or unpaired *t* test (Prism version 5.0, GraphPad). All statistical tests were two-tailed. *P* values of <0.05 were considered to indicate statistical significance.

Results

The inhibitory effects of DEX on spontaneous action potentials in SA node cells

The effect of DEX on SA node automaticity was examined using the amphotericin B-perforated patch-clamp technique. DEX was administered to a SA node cell at concentrations of 5 nM, 10 nM, 100 nM and 1 μM for approximately 2-3 min until it was ensured that it had reached a steady state. The firing rate of spontaneous action potentials was decreased by each concentration of DEX (Figure 1A). Figure 1B shows the spontaneous action potentials illustrated on an expanded time scale before and during exposure to DEX, and the washout results. At concentrations of ≥10 nM, DEX significantly reduced the firing rate (Figure 1C). It is well-known that the slope of the diastolic depolarization, namely the diastolic depolarization rate (DDR), plays an important role in determining the firing rate of the SA node.[26] As shown in Figure 1D, the DDR was also significantly during the administration of 10 nM, 100 nM and 1 μM DEX, respectively. Table 1 shows the parameters of the action potentials, including the action potential amplitude (APA), maximum diastolic potential (MDP), action potential duration at 50% and 90% (APD_{50} and APD_{90}) and the maximal rate of the action potential depolarization (max dV/dt).

Inhibitory effects of I_f current in SA node cells

To investigate the ionic contribution of the inhibitory action of DEX on the spontaneous activity of SA node cells, we investigated the effect of DEX on various pacemaker-related ion currents, including I_f, I_{Kr}, I_{Ks}, $I_{Ca,L}$, I_{NCX} and $I_{K,ACh}$.

Firstly, the reversal potential of I_f was measured by tail currents at various test potentials between 10 and -50 mV for 2 s in the absence and presence of DEX (1 μM). Tail currents were plotted against the test potential, with fitting of lines by linear regression. The reversal potential was not changed in the presence of DEX (control, -32.5 ± 5.7 mV; DEX, -33.11 ± 3.6 mV (n = 3, N = 2)). Figure 2A illustrates the superimposed current traces of I_f activated at test potentials of -50 to -140 mV during the administration of 100 nM DEX. DEX decreased the amplitude of I_f in a dose-dependent manner, as shown in the conductance-voltage relationship curves fitted with the Boltzmann equation (Figure 2B). Maximal conductance at -140 mV (Figure 2C) was significantly reduced by exposure to 10 nM, 100 nM and 1 μM DEX. We then evaluated the voltage dependence of the I_f activation with normalized conductance-voltage relationships. DEX at various concentrations (Figure 2D) caused a significant shift in the voltage-dependence of channel activation to more negative potentials. Importantly, DEX markedly decreased the amplitude of I_f at physiological potential ranges

relevant to pacemaker depolarization at -70 mV (Figure 2E). In addition, we demonstrated that ivabradine, a selective I_f antagonist, markedly inhibited the time-dependent activation of I_f current (Figure 2E). The time-dependent activating component of I_f was thus calculated to determine the percentage inhibition induced by DEX at -70 mV (Figure 2F).

Figure 3A shows the time course of I_f activation at -140 mV fitted by the sum of two exponential functions in the absence and presence of 1 μM DEX. Each concentration of DEX increased the fast activation time constant (Figure 3B), while the slow activation time constant was increased by 100 nM and 1 μM DEX (Figure 3C). The relative amplitude of the fast component of I_f activation was not affected by the respective concentrations of DEX (Figure 3D).

The effects of DEX on pacemaker-related ion currents I_{Kr}, I_{Ks}, $I_{Ca,L}$, I_{NCX} and $I_{K,ACh}$ in SA node cells

I_{Kr} was determined as E-4031 (I_{Kr} selective antagonist)-sensitive difference current in the present experiment. Supplemental Figure 1A shows superimposed current traces during 250-ms depolarizing steps to 0 mV applied from a holding potential of -50 mV during exposure to 1 μM DEX. The amplitudes of the I_{Kr} tail currents at test potentials of -40 to +50

mV were plotted and fitted with the Boltzmann equation (Supplemental Figure 1B). There was no significant difference in the maximal amplitudes of the I_{Kr} tail currents between control cells and cells exposed to 1 μM DEX (Supplemental Figure 1C).

I_{Ks} current was activated by 2-s depolarizing steps applied from a holding potential of -50 mV to test potentials of -40 mV to +50 mV during control and the exposure to 1 μM DEX (Supplemental Figure 2A). DEX did not induce a significant difference in the maximal amplitude of I_{Ks} tail current (Supplemental Figure 2B and C).

$I_{Ca,L}$ was evaluated using depolarizing steps to -10 mV applied from a holding potential of -50 mV. The amplitude $I_{Ca,L}$ was measured at 8 min and at 13 min after start of the experiments in the absence and presence of 1 μM DEX, respectively (Supplemental Figure 3A and B). DEX did not significantly affect the slight declines in the $I_{Ca,L}$ amplitude between 8 min and 13 min (Supplemental Figure 3C).

To evaluate the effect of I_{NCX}, we recorded membrane currents before and during the administration of DEX, and after washout, then exposed cells to $NiCl_2$ to block the I_{NCX} (Supplemental Figure 4A). DEX (1 μM) did not affect the membrane currents during voltage ramping between +40 mV and -120 mV. Supplemental Figure 4B and C show the current-voltage relationship for I_{NCX}, indicating that DEX does not influence the activity of

I_{NCX}.

In the present experiment, the reduction in firing rate of action potentials was accompanied by a tendency for hyperpolarization of MDP. In general, $I_{K,ACh}$ is activated by the stimulation of muscarinic receptors and then hyperpolarizes MDP, leading to a decrease in spontaneous activity.[26] As shown in Supplemental Figure 5A, membrane currents were recorded before and during exposure to 1 μM DEX and 1 μM ACh, respectively. ACh markedly increased membrane currents, while DEX did not alter the currents. The evaluation of the current-voltage relationships of the membrane current and $I_{K,ACh}$ current further demonstrated that DEX has no effect on $I_{K,ACh}$ (Supplemental Figure 5B and C).

The negative chronotropic effects of DEX on spontaneous action potentials in SA node cells mediated via I_1R activation

We next investigated whether both α_2-AR and IR are involved in the DEX-induced inhibition in SA node cells. In the presence of 1 μM yohimbine, an α_2-AR antagonist, the firing rate of spontaneous action potentials was still reduced by different concentrations of DEX (10 nM, 100 nM and 1 μM) (Figure 4A), indicating that yohimbine did not alter the reduction of the firing rate induced by DEX (Figure 4C). In contrast, efaroxan (10 μM), an antagonist of

α_2-AR and IR, and especially the imidazoline I_1 receptor (I_1R), attenuated the DEX-induced inhibition of spontaneous automaticity (Figure 4B and D). Similar to efaroxan, idazoxan (10 μM), another antagonist of α_2-AR and IR, also markedly reduced the inhibitory effect of 1 μM DEX (Figure 4E). These results suggest that DEX decreases the spontaneous automaticity via I_1R rather than via the α_2-AR signaling pathway.

Previous reports showed that DEX activates the protein kinase C (PKC) via the I_1R signaling pathway.[27] We therefore examined the influence of BIS-I, a PKC antagonist, on the inhibitory effect of DEX on the firing rate. As shown in Figure 5A, BIS-I (200 nM) did not affect the DEX-induced inhibitory effect. In addition, PMA (100 nM), a PKC activator, did not cause any change in the spontaneous automaticity (Figure 5B). These results indicate that the PKC pathway is irrelevant to the firing rate inhibition induced by DEX.

Impairment of the I_f function in SA node cells induced by DEX via the I_1R signaling pathway

To examine whether DEX could attenuate I_f current via I_1R activation, efaroxan (10 μM) was administered for 5 min, then cells were exposed to DEX (1 μM) for 5 min. As demonstrated in Figure 6, although efaroxan slightly decreased the amplitude of I_f, DEX did not cause any

further reduction in the presence of efaroxan (Figure 6A, B and C). Furthermore, the voltage-dependence and time course of the channel activation were not changed by treatment with DEX in the presence of efaroxan (Figure 6 D and E).

The inhibitory effect of imidazoline-related agonists on spontaneous action potentials and I_f current in SA node cells

To further confirm the involvement of I_1R activation in the DEX-induced negative chronotropic effects on spontaneous automaticity, moxonidine, an α_2-AR and I_1R agonist with a higher selectivity to I_1R than DEX, was administered to SA node cells at concentrations of 100 nM and 1 μM. Each concentration of moxonidine reduced the firing rate of spontaneous action potentials (Figure 7A and B). In addition, we also examined the effects of moxonidine and another I_1R-related agonist rilmenidine on the activity of I_f current. Figure 7C and D illustrate the superimposed current traces of I_f before and during exposure to 1 μM moxonidine and 1 μM rilmenidine, respectively. The conductance-voltage relationships for I_f show that both moxonidine and rilmenidine significantly decreased the amplitude of I_f (Figure 7E and F) and caused a significant shift in the voltage-dependent activation of I_f to more negative potentials (Figure 7G). Furthermore, moxonidine and rilmenidine reduced the

I_f activity at -70 mV by 43.9% ± 5.2% and 37.5% ± 7.7%, respectively.

Discussion

The present study indicates that DEX has a negative chronotropic effect on the spontaneous action potentials of SA node cells in guinea pigs. Our findings show that (1) DEX induced a decrease in the firing rate of spontaneous action potentials via the I_1R signaling pathway; (2) DEX significantly reduced the amplitude of I_f, even within the physiological pacemaker potential range; (3) DEX evoked a shift in the voltage-dependence of channel activation to more negative potentials and a deceleration in the channel activation rate; (4) DEX had no effect on pacemaker-associated ion channels, including I_{Kr}, I_{Ks}, $I_{Ca,L}$, I_{NCX} and $I_{K,ACh}$.

Involvement of I_1R activation in DEX-induced negative chronotropic effects on the spontaneous automaticity in SA node cells

It is known that I_1R is located in the brain, heart, kidney and pancreas.[13] Although the protein expression levels of I_1R and α_2-AR in the SA node have not been clarified, the expression of α_2-AR was confirmed at the mRNA level in human left ventricular tissue,[28] whereas the protein level of I_1R in human ventricles was demonstrated based on an immunoblot analysis.[29] Additionally, DEX could functionally bind these two receptors in the rat myocardium.[17] It is known that α_2-AR binds G_i-protein and then inhibits the production of

cAMP from ATP by impairing adenylyl cyclase activity.[30] We presumed that DEX might suppress SA node automaticity via α_2-AR activation; however, the present results showed that the inhibitory effect of DEX on the spontaneous action potentials is attenuated by efaroxan and idazoxan, α_2-AR and I_1R antagonists, respectively, but not by yohimbine, an α_2-AR antagonist, suggesting that DEX suppresses SA node automaticity via the I_1R signaling pathway other than the α_2-AR signaling pathway. Related to this finding, we further demonstrated that moxonidne, an I_1R agonist more selective than DEX, also decreased the firing rate of spontaneous action potentials. Our results are supported by previous studies, which reported that the DEX-induced reduction in the firing rate in the rabbit SA node was not totally mediated by the α_2-AR signaling pathway.[16] Furthermore, it was demonstrated that the hypotension and bradycardia induced by the suppression of the sympathetic neurons through RVLM have a stronger association with I_1R than α_2-AR.[31] The result suggests that DEX might regulate the sympathetic activity via not only by the α_2-AR signaling pathway but also via the I_1R signaling pathway. Thus, we consider that the activation of I_1R plays an important role in the functional modulation of the SA node and sympathetic neurons.

The I_f function in SA node and its reduction induced by DEX via the I_1R signaling

pathway

The I_f channel is known to partly contribute to the regulation of the rate of automaticity in SA node cells, because the opening of the I_f channel facilitates the formation of the "pacemaker potential" up to the threshold of Ca^{2+} channel activation.[32] An increase in intracellular cAMP could accelerate the increase in the pacemaker potential by shifting the voltage dependence of the I_f channels to a more positive potential.[26,32] This phenomenon is considered to be an explanation for the positive chronotropic effect of *β*-adrenergic receptor agonist in the heart.[33] In the present study, DEX (1 μM) inhibited I_f current by 52%, with a resultant reduction in the spontaneous beating rate by 32%. Our result is similar to a previous report showing that ivabradine (3 μM) inhibited I_f current by 34% and reduced the spontaneous action potentials by approximately 13% in the rabbit SA node.[34] In rat paraventricular nucleus parvocellular neurons, DEX is reported to inhibit I_f current by decreasing the current amplitude and inducing a slight shift in the voltage-dependence of channel activation to negative potentials via α_2-AR.[35]

As demonstrated in the present study, DEX significantly reduced I_f via I_1R but not α_2-AR activation. In addition, two other drugs (moxonidine and rilmenidine) with a higher selectivity to I_1R also reduced I_f current, as expected. Our results suggest that DEX might

inhibit SA node automaticity in guinea pigs by decreasing the I_f channel activity, mainly through the I_1R signaling pathway. It is noteworthy that ligands for I_1R decreased the cAMP activity in rat striatal medium spiny neurons[36] and rat pheochromocytoma (PC12) cells.[37] Because cAMP facilitates I_f current activity[33] and the basal cAMP concentration in the SA node is higher than in other myocytes,[38] the cAMP activity may be associated with the DEX-induced inhibition of I_f via the activation of I_1R. However, further study is required to test this hypothesis.

PKC activation is not required for DEX-induced negative chronotropic effects

We also examined the intracellular signal transduction for the action of DEX via I_1R activation. Several reports reported that I_1R in PC12 cells activates the PKC pathway[39] and that presynaptic I_1R suppresses postsynaptic currents by PKC activation in the spiny neurons in rat striatal medium.[36] In mouse hippocampal slices, the activation of I_1R by DEX has a nerve protective action through the PKC pathway, which involves the extracellular signal-regulated kinase.[27] However, in the present study, a specific antagonist, BIS-1, and a specific activator, PMA, did not affect the DEX-induced negative chronotropic effect on the spontaneous action potentials in SA node cells, indicating that the PKC activation pathway is

not required for the DEX-induced inhibition of SA node automaticity.

No effects of DEX on other pacemaker-related ion currents

There have been some reports on the effects of DEX on K^+ channels. In rat paraventricular nucleus magnocellular neurons, DEX activated G protein-coupled inwardly rectifying K^+ current.[35] In addition, DEX suppressed delayed rectifier K^+ current in rat cerebellar granule cells and NG108-15 neuronal cells, a hybrid of mouse neuroblastoma and rat glioma cells.[40] Moreover, DEX is reported to protect the heart function from ischemia reperfusion injury by activating the Ca^{2+}-sensitive K^+ channels.[41] It is well known that $I_{Ca,L}$ plays an important role in pacemaker activity.[26] A previous report showed that DEX inhibits $I_{Ca,L}$ in rat ventricular myocytes, partially through the activation of α_2-AR;[42] however, another study showed that DEX had no effect on $I_{Ca,L}$ in NG108-15 neuronal cells.[40] Our findings provide evidence to support that DEX, even at higher concentrations, could not affect the I_{Kr}, I_{Ks}, $I_{K,Ach}$ or $I_{Ca,L}$ channel activity in SA node cells. The reasons for these discrepancies are not clear; however, they are probably related to tissue- and species-specific factors.

Clinical significance of DEX-induced negative chronotropic action

Our experiment demonstrated that clinically relevant concentrations (≤10 nM) of DEX slowed the spontaneous firing rate in SA node cells, which is associated with a marked reduction in the I_f channel activity at physiological pacemaker potentials. In clinical usage, the heart rate is considered to show a greater decrease, because sympathetic neurons are simultaneously depressed, in addition to the direct inhibition of the SA node function. Above all, in the elderly,[43] individuals with heart failure[44] or individuals with familial sinus bradycardia,[45,46] in whom I_f current is decreased, it is necessary to use DEX cautiously due to the high risk that the drug will have a stronger effect on the SA node function. Because several anesthetics, including sevoflurane,[25] desflurrane[19] and propofol[20] can also inhibit the I_f channel, when these anesthetics are used in combination, the I_f channel is considered to be more seriously impaired. Moreover, we showed that DEX inhibits the heart rate in a concentration-dependent manner and that the administration of an overdose or bolus injection should be avoided, even in patients without serious complications.

Limitations

Several limitations associated with the present study warrant mention. The limitations of the present study are as follows: (1) the regulatory mechanisms of spontaneous automaticity in

SA node cells might differ between experimental animals and humans, making it difficult to directly extrapolate our data obtained from guinea pigs to the SA node function of human; (2) the distribution and function of the imidazoline receptor in the human heart (especially the SA node) have not been fully investigated and should be clarified in a future study; (3) selective agonists and antagonists of the imidazoline receptor have not yet been developed, so the development of these drugs and experiments with them are required; (4) the heart rate is controlled not only by the SA node but also by the sympathetic and parasympathetic nerves. However, the effect of DEX regarding the function of the autonomic nerve system was not examined in the present study; (5) the spontaneous automaticity of the SA node is modeled as two clocks for a better interpretation of its function—the "membrane voltage clock" and the "calcium clock"—with the membrane voltage clock induced by I_f and other inward currents, such as T-type Ca^{2+} current and Na^+/Ca^{2+} exchange current, while the calcium clock is induced by rhythmic Ca^{2+} release from the sarcoplasmic reticulum.[47] The further investigation of DEX-induced modulation on the calcium clock function is needed to test this hypothesis.

Conclusion

We demonstrated that DEX at relevant clinical doses results in a negative chronotropic effect on SA node automaticity by reducing the I_f channel activity through the I_1R signaling pathway but not the α_2-AR signaling pathway. The present study suggests that I_1R activation may play a crucial role in the modulation of the SA node and the sympathetic neuron functions.

Author contribution

M.I and H.M participated in the research design. M.I and H.M conducted the experiments. M.I, W-G.D, A.K, H.M and H.K performed the data analysis. M.I, W-G.D and H.M wrote the manuscript. All authors revised the final version of manuscript and approved its submission.

References

1. Mantz J, Josserand J, Hamada S. Dexmedetomidine: new insights. Eur J Anaesthesiol. 2011;28(1):3-6.

2. Ebert TJ, Hall JE, Barney JA, Uhrich TD, Colinco MD. The effects of increasing plasma concentrations of dexmedetomidine in humans. Anesthesiology. 2000;93(2):382-94.

3. Colin PJ, Hannivoort LN, Eleveld DJ, Reyntjens KMEM, Absalom AR, Vereecke HEM, et al. Dexmedetomidine pharmacodynamics in healthy volunteers: 2. Haemodynamic profile. Br J Anaesth. 2017;119(2):211-20.

4. Tan JA, Ho KM. Use of dexmedetomidine as a sedative and analgesic agent in critically ill adult patients: a meta-analysis. Intensive Care Med. 2010;36(6):926-39.

5. Shuplock JM, Smith AH, Owen J, Van Driest SL, Marshall M, Saville B, et al. Association between perioperative dexmedetomidine and arrhythmias after surgery for congenital heart disease. Circ Arrhythm Electrophysiol. 2015;8(3):643-50.

6. Geng J, Qian J, Cheng H, Ji F, Liu H. The Influence of Perioperative Dexmedetomidine on Patients Undergoing Cardiac Surgery: A Meta-Analysis. PLoS One. 2016;11(4):e0152829.

7. Ingersoll-Weng E, Manecke GR, Thistlethwaite PA. Dexmedetomidine and cardiac arrest. Anesthesiology. 2004;100(3):738-9.

8. Patel VJ, Ahmed SS, Nitu ME, Rigby MR. Vasovagal syncope and severe bradycardia following intranasal dexmedetomidine for pediatric procedural sedation. Paediatr Anaesth. 2014;24(4):446-8.

9. Webb CA, Weyker PD, Flynn BC: Asystole after orthotopic lung transplantation: examining the interaction of cardiac denervation and dexmedetomidine. Case Rep Anesthesiol. 2012; 2012:203240.

10. Hongo M, Fujisawa S, Adachi T, Shimbo T, Shibata S, Ohba T, et al. Age-related effects of dexmedetomidine on myocardial contraction and coronary circulation in isolated guinea pig hearts. J Pharmacol Sci. 2016;131(2):118-25.

11. Kubo T, Goshima Y, Hata H, Misu Y. Evidence that endogenous catecholamines are involved in alpha 2-adrenoceptor-mediated modulation of the aortic baroreceptor reflex in the nucleus tractus solitarii of the rat. Brain Res. 1990;526(2):313-7.

12. Shirasaka T, Qiu DL, Kannan H, Takasaki M. The effects of centrally administered dexmedetomidine on cardiovascular and sympathetic function in conscious rats. Anesth Analg. 2007;105(6):1722-8.

13. Lowry JA, Brown JT. Significance of the imidazoline receptors in toxicology. Clin Toxicol (Phila). 2014;52(5):454-69.

14. Brede M, Philipp M, Knaus A, Muthig V, Hein L. alpha2-adrenergic receptor subtypes - novel functions uncovered in gene-targeted mouse models. Biol Cell. 2004;96(5):343-8.

15. Hammer GB, Drover DR, Cao H, Jackson E, Williams GD, Ramamoorthy C, et al. The effects of dexmedetomidine on cardiac electrophysiology in children. Anesth Analg. 2008;106(1):79-83.

16. Pan X, Zhang Z, Huang YY, Zhao J, Wang L. Electrophysiological Effects of Dexmedetomidine on Sinoatrial Nodes of Rabbits. Acta Cardiol Sin. 2015;31(6):543-9.

17. Yoshikawa Y, Hirata N, Kawaguchi R, Tokinaga Y, Yamakage M. Dexmedetomidine Maintains Its Direct Cardioprotective Effect Against Ischemia/Reperfusion Injury in Hypertensive Hypertrophied Myocardium. Anesth Analg. 2018;126(2):443-52.

18. Xie Y, Ding WG, Matsuura H. Ca2+/calmodulin potentiates I Ks in sinoatrial node cells by activating Ca2+/calmodulin-dependent protein kinase II. Pflugers Arch. 2015;467(2):241-51.

19. Kojima A, Ito Y, Kitagawa H, Matsuura H, Nosaka S. Direct negative chronotropic action of desflurane on sinoatrial node pacemaker activity in the guinea pig heart. Anesthesiology. 2014;120(6):1400-13.

20. Kojima A, Ito Y, Kitagawa H, Matsuura H. Ionic mechanisms underlying the negative chronotropic action of propofol on sinoatrial node automaticity in guinea pig heart. Br J Pharmacol. 2015;172(3):799-814.

21. Wu J, Schuessler RB, Rodefeld MD, Saffitz JE, Boineau JP. Morphological and membrane characteristics of spider and spindle cells isolated from rabbit sinus node. Am J Physiol Heart Circ Physiol. 2001;280(3):H1232-40.

22. Toyoda F, Ding WG, Matsuura H. Heterogeneous functional expression of the sustained inward Na. Pflugers Arch. 2018;470(3):481-90.

23. Ding WG, Toyoda F, Matsuura H. Blocking action of chromanol 293B on the slow component of delayed rectifier K(+) current in guinea-pig sino-atrial node cells. Br J Pharmacol. 2002;137(2):253-62.

24. Mangoni ME, Nargeot J. Properties of the hyperpolarization-activated current (I(f)) in isolated mouse sino-atrial cells. Cardiovasc Res. 2001;52(1):51-64.

25. Kojima A, Kitagawa H, Omatsu-Kanbe M, Matsuura H, Nosaka S. Inhibitory effects of sevoflurane on pacemaking activity of sinoatrial node cells in guinea-pig heart. Br J Pharmacol. 2012;166(7):2117-35.

26. Mangoni ME, Nargeot J. Genesis and regulation of the heart automaticity. Physiol Rev. 2008;88(3):919-82.

27. Dahmani S, Rouelle D, Gressens P, Mantz J. Characterization of the postconditioning effect of dexmedetomidine in mouse organotypic hippocampal slice cultures exposed to oxygen and glucose deprivation. Anesthesiology. 2010;112(2):373-83.

28. Berkowitz DE, Price DT, Bello EA, Page SO, Schwinn DA. Localization of messenger RNA for three distinct alpha 2-adrenergic receptor subtypes in human tissues. Evidence for species heterogeneity and implications for human pharmacology. Anesthesiology. 1994;81(5):1235-44.

29. El-Ayoubi R, Gutkowska J, Regunathan S, Mukaddam-Daher S. Imidazoline receptors in the heart: characterization, distribution, and regulation. J Cardiovasc Pharmacol. 2002;39(6):875-83.

30. Wang J, Gareri C, Rockman HA. G-Protein-Coupled Receptors in Heart Disease. Circ Res. 2018;123(6):716-35.

31. Li G, Wang X, Abdel-Rahman AA. Neuronal norepinephrine responses of the rostral ventrolateral medulla and nucleus tractus solitarius neurons distinguish the I1- from the alpha2-receptor-mediated hypotension in conscious SHRs. J Cardiovasc Pharmacol. 2005;46(1):52-62.

32. Biel M, Schneider A, Wahl C. Cardiac HCN channels: structure, function, and modulation. Trends Cardiovasc Med. 2002;12(5):206-12.

33. DiFrancesco D, Tortora P. Direct activation of cardiac pacemaker channels by intracellular cyclic AMP. Nature. 1991;351(6322):145-7.

34. Yaniv Y, Maltsev VA, Ziman BD, Spurgeon HA, Lakatta EG. The "funny" current (I(f)) inhibition by ivabradine at membrane potentials encompassing spontaneous depolarization in pacemaker cells. Molecules. 2012;17(7):8241-54.

35. Shirasaka T, Kannan H, Takasaki M. Activation of a G protein-coupled inwardly rectifying K+ current and suppression of Ih contribute to dexmedetomidine-induced inhibition of rat hypothalamic paraventricular nucleus neurons. Anesthesiology. 2007;107(4):605-15.

36. Tanabe M, Kino Y, Honda M, Ono H. Presynaptic I1-imidazoline receptors reduce GABAergic synaptic transmission in striatal medium spiny neurons. J Neurosci. 2006;26(6):1795-802.

37. Greney H, Ronde P, Magnier C, Maranca F, Rascente C, Quaglia W, et al. Coupling of I(1) imidazoline receptors to the cAMP pathway: studies with a highly selective ligand, benazoline. Mol Pharmacol. 2000;57(6):1142-51.

38. Vinogradova TM, Lyashkov AE, Zhu W, Ruknudin AM, Sirenko S, Yang D, et al. High basal protein kinase A-dependent phosphorylation drives rhythmic internal Ca2+ store oscillations and spontaneous beating of cardiac pacemaker cells. Circ Res. 2006;98(4):505-14.

39. Edwards L, Fishman D, Horowitz P, Bourbon N, Kester M, Ernsberger P. The I1-imidazoline receptor in PC12 pheochromocytoma cells activates protein kinases C,

extracellular signal-regulated kinase (ERK) and c-jun N-terminal kinase (JNK). J Neurochem. 2001;79(5):931-40.

40. Chen BS, Peng H, Wu SN. Dexmedetomidine, an alpha2-adrenergic agonist, inhibits neuronal delayed-rectifier potassium current and sodium current. Br J Anaesth. 2009;103(2):244-54.

41. Behmenburg F, Pickert E, Mathes A, Heinen A, Hollmann MW, Huhn R, et al. The Cardioprotective Effect of Dexmedetomidine in Rats Is Dose-Dependent and Mediated by BKCa Channels. J Cardiovasc Pharmacol. 2017;69(4):228-35.

42. Zhao J, Zhou CL, Xia ZY, Wang L. Effects of Dexmedetomidine on L-Type Calcium Current in Rat Ventricular Myocytes. Acta Cardiol Sin. 2013;29(2):175-80.

43. Larson ED, St Clair JR, Sumner WA, Bannister RA, Proenza C. Depressed pacemaker activity of sinoatrial node myocytes contributes to the age-dependent decline in maximum heart rate. Proc Natl Acad Sci U S A. 2013;110(44):18011-6.

44. Verkerk AO, Wilders R, Coronel R, Ravesloot JH, Verheijck EE. Ionic remodeling of sinoatrial node cells by heart failure. Circulation. 2003;108(6):760-6.

45. Milanesi R, Baruscotti M, Gnecchi-Ruscone T, DiFrancesco D. Familial sinus bradycardia associated with a mutation in the cardiac pacemaker channel. N Engl J Med. 2006;354(2):151-7.

46. Nof E, Luria D, Brass D, Marek D, Lahat H, Reznik-Wolf H, et al. Point mutation in the HCN4 cardiac ion channel pore affecting synthesis, trafficking, and functional expression is associated with familial asymptomatic sinus bradycardia. Circulation. 2007;116(5):463-70.

47. Lakatta EG, Maltsev VA, Vinogradova TM. A coupled SYSTEM of intracellular Ca2+ clocks and surface membrane voltage clocks controls the timekeeping mechanism of the heart's pacemaker. Circ Res. 2010;106(4):659-73.

Figure Legends

Figure 1

The effect of dexmedetomidine (DEX) on the firing rate of spontaneous action potentials in guinea pig SA node cells. A, Continuous recording of spontaneous action potentials during the administration of DEX at concentrations of 5 nM, 10 nM, 100 nM and 1 μM (upper panel). The simultaneous measurement of the spontaneous firing rate plotted on the same time scale (lower panel). B, Spontaneous action potentials on an expanded time scale recorded at the time points indicated by the characters (a-f) in panel A. C and D, The spontaneous firing rate (C) and diastolic depolarization rate (DDR) (D) before (control) and during the administration of DEX at each concentration (n = 10-18, N = 9). These data were analyzed by a one-way ANOVA followed by Dunnett's test. *P < 0.05 in comparison to control.

Figure 2

Dexmedetomidine (DEX) induced a decrease in the conductance of I_f and a hyperpolarizing shift of channel activation. A, Superimposed current traces of I_f activated during 2-s hyperpolarizing steps from a holding potential of -40 mV to test potentials of -50 mV to -140

mV, before (control) and during the administration of 100 nM DEX for 5 min. B, The conductance (g_f)-voltage relationship for I_f constructed using the reversal potential of -31 mV in the absence (control) and presence of DEX at each concentration (10 nM, 100 nM and 1 μM, fitted with the Boltzmann equation (n = 7-9, N = 8). C, Maximal conductance of I_f ($g_{f,max}$) obtained from fitting with the Boltzmann equation (n = 7-9, N = 8). D, The voltage at half-maximal activation (V_h) obtained by fitting the conductance-voltage relationship to the Boltzmann equation in the absence and presence of DEX (n = 7-9, N = 8). E, I_f current at a test potential -70 mV before and during the administration of 1 μM DEX or 30 μM ivabradine. F, The percent inhibition of I_f at -70 mV induced by DEX at concentrations of 10 nM, 100 nM and 1 μM (n = 7-9, N = 8). These data were analyzed by a paired t test. *P < 0.05 in comparison to control.

Figure 3

The effect of dexmedetomidine (DEX) on the activation rate of I_f current. A, I_f activated during 2-s hyperpolarizing steps to -140 mV from a holding potential of -40 mV, before (control) and during the administration of 1 μM DEX, which was fitted with two exponential functions. The right traces show superimposed I_f, where the peak amplitude of I_f in the

presence of DEX was normalized to that of control to define the slowing of I_f activation. B, C, The activation time constants for the fast (τ_{fast}, B) and the slow (τ_{slow}, C) components at -140 mV in the absence and presence of different concentrations of DEX (10 nM, 100 nM and 1 μM, n = 7-9, N = 8). D, The relative amplitude of the fast component of I_f activation at -140 mV in the absence and presence of DEX (n = 7-9, N = 8). These data were analyzed by a paired t test. *$P < 0.05$ in comparison to control.

Figure 4

The attenuation of dexmedetomidine (DEX)-induced inhibition of spontaneous action potentials in SA node cells by the α_2-AR and I_1R antagonists (efaroxan and idazoxan). A, Continuous recording of action potentials during the administration of DEX at concentrations of 10, 100 nM, and 1 μM in the presence of yohimbine (YOH, 1 μM), an α_2-AR antagonist (upper panel). The simultaneous measurement of the spontaneous firing rate plotted on the same time scale (lower panel). B, The continuous recording of action potentials during the administration of DEX at concentrations of 10, 100 nM, and 1 μM, in the presence of 10 μM efaroxan (EFA, 10 μM, upper panel). The simultaneous measurement of the spontaneous firing rate plotted on the same time scale (lower panel). C, The percent reduction in the firing

rate induced by DEX in the absence and presence of YOH (n = 8-9, N = 6). D, The percent reduction in the firing rate induced by DEX in the absence and presence of EFA (n = 10, N = 5). E, The percent reduction in the firing rate induced by DEX in the absence and presence of idazoxan (IDA, 10 μM) (n = 7, N =3). Note that the data in the absence of YOH and EFA shown in panels C, D and E were obtained from the same data shown in Figure 1. These data were analyzed by an unpaired t test. *$P < 0.05$ in comparison to control.

Figure 5

Protein kinase C (PKC) failed to suppress the effect of dexmedetomidine (DEX) on spontaneous action potentials in SA node cells. A, The percent reduction in firing rate induced by DEX in the absence and presence of a PKC inhibitor, bisindolylmaleimide I (BIS-I, 200 nM) (n = 6, N = 4). Note that the data in the absence of BIS-I were obtained from the control data shown in Figure 1. The data were analyzed by an unpaired t test. B, The firing rate before and during the administration of phorbol 12-myristate 13-acetate (PMA, 100 nM), a PKC activator, for more than 5 min (n = 7, N = 4). The data were analyzed by a paired t test.

Figure 6

The attenuation of dexmedetomidine (DEX)-induced impairment of I_f current by efaroxan (EFA). A, Superimposed current traces of I_f activated during 2-s hyperpolarizing steps from a holding potential of -40 mV to test potentials of -50 mV to -140 mV, before (control) and during the administration of 1 μM DEX for 5 min (upper panel). The lower panel shows superimposed current traces of I_f activated during the same hyperpolarizing steps, before and during the administration of 10 μM EFA and EFA plus 1 μM DEX for 5 min, respectively. B, Comparison of the maximal conductance of I_f ($g_{f,max}$) by fitting the conductance-voltage relationship to a Boltzmann equation in the absence (control) and presence of EFA and EFA plus DEX (n = 5, N =3). C, The percent inhibition of I_f induced by DEX at -70 mV in the absence and presence of EFA (n = 5-9, N = 3). Note that the data in the absence of EFA were obtained from the same data shown in Figure 2. D, The voltage at half-maximal activation (V_h) obtained by a Boltzmann fitting in the absence (control) and presence of EFA and EFA plus DEX (n = 5, N = 3). E, The time constants for the fast (τ_{fast}, left panel), and slow (τ_{slow}, middle panel) components of I_f activation at -140 mV obtained by fitting with two exponential functions before (control) and during the administration of EFA and EFA plus DEX. The right panel shows the relative amplitude of the fast component

(n = 5, N = 3). The data concerning the $g_{f,max}$, V_h and time constants were analyzed by a paired t test, control vs. EFA and EFA vs. EFA+DEX, respectively. The data concerning the percent inhibition were analyzed by an unpaired t test.

Figure 7

The effect of moxonidine on the firing rate of spontaneous action potentials and I_f current. A, Continuous recording of the spontaneous action potentials during administration of moxonidine (MOX) at concentrations of 100 nM and 1 μM (upper panel). The simultaneous measurement of the spontaneous firing rate plotted on the same time scale (lower panel). B, The spontaneous firing rate before (control) and during the administration of MOX at each concentration (n = 6-9, N = 4). The data were analyzed by a one-way ANOVA followed by Dunnett's test. C, Superimposed current traces of I_f activated during 2-s hyperpolarizing steps from a holding potential of -40 mV to test potentials of -50 to -140 mV before (control) and during the administration of 1 μM MOX for 5 min. D, Superimposed current traces of I_f activated by the same protocol, before (control) and during the administration of 1 μM rilmenidine (RIL) for 5 min. E, The conductance (g_f)-voltage relationship for I_f constructed using the reversal potential of -31 mV in the absence (control) and presence of

1 μM MOX (n = 8, N = 3) and 1 μM RIL (n = 8, N = 3), fitted with the Boltzmann equation. F, Comparison of the maximal conductance of I_f ($g_{f,max}$) by fitting the conductance-voltage relationship to a Boltzmann equation in the absence (control) and presence of MOX (n = 8, N = 3) and RIL (n = 8, N = 3). G, The voltage at half-maximal activation (V_h) obtained by a Boltzmann fitting in the absence (control) and presence of MOX (n = 8, N = 3) and RIL (n = 8, N = 3). The data of $g_{f,max}$ and V_h were analyzed by a paired t test. *P < 0.05 in comparison to control.

Figure 1

Click here to access/download;Figure;Mariko Ishihara et al-Figure1.tif

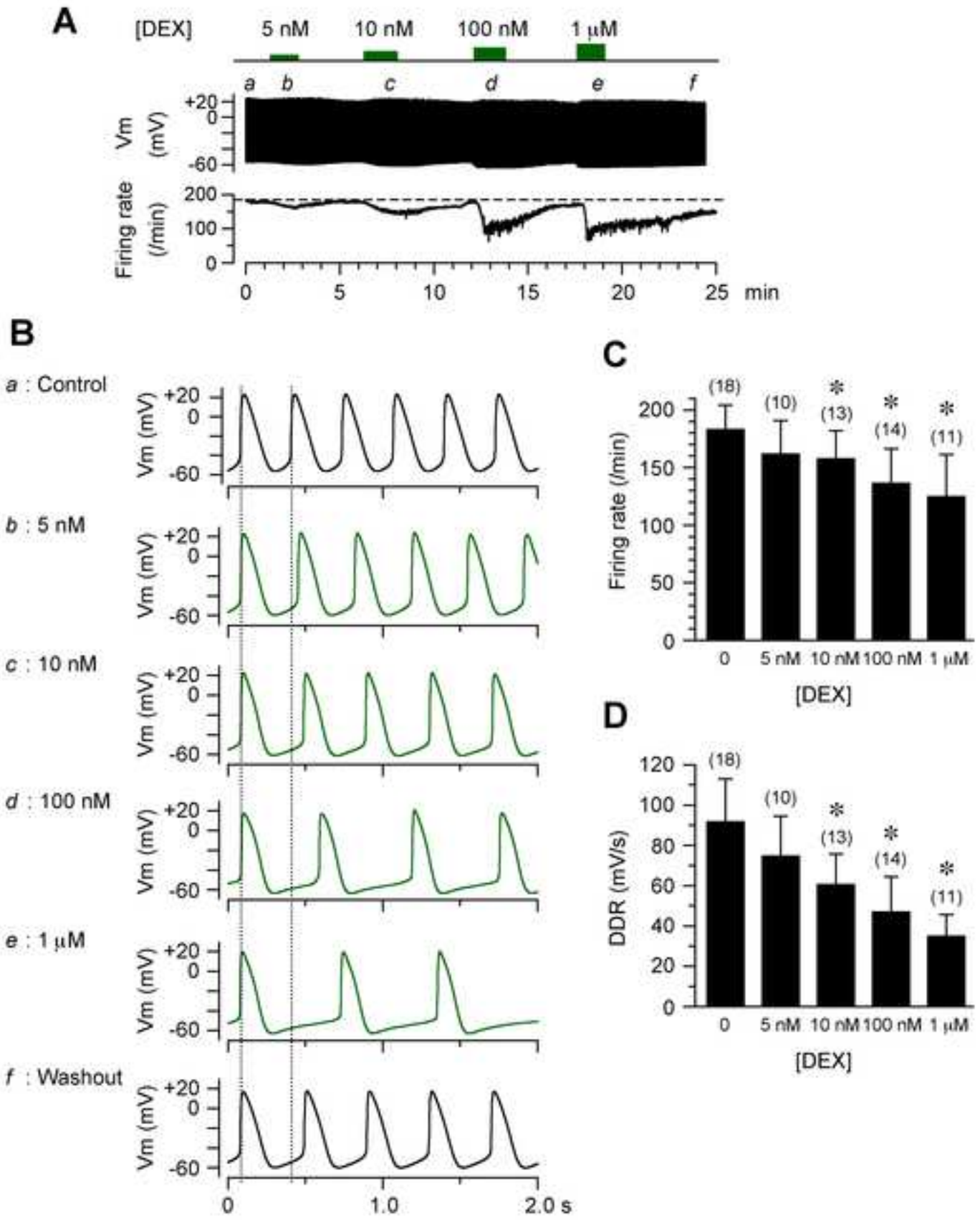

Figure 2

Click here to access/download;Figure;Mariko Ishihara et al-Figure2.tif

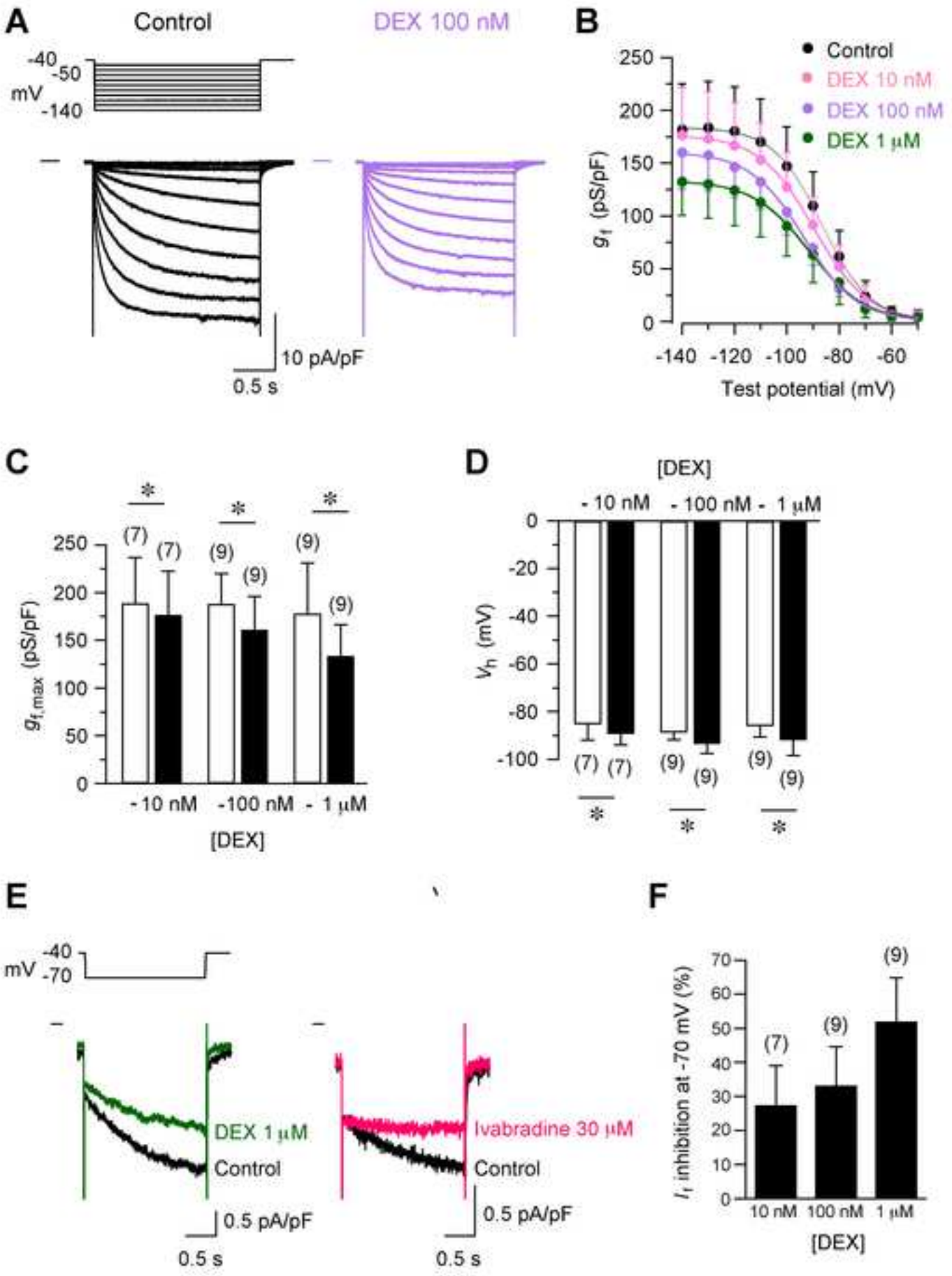

Figure 3

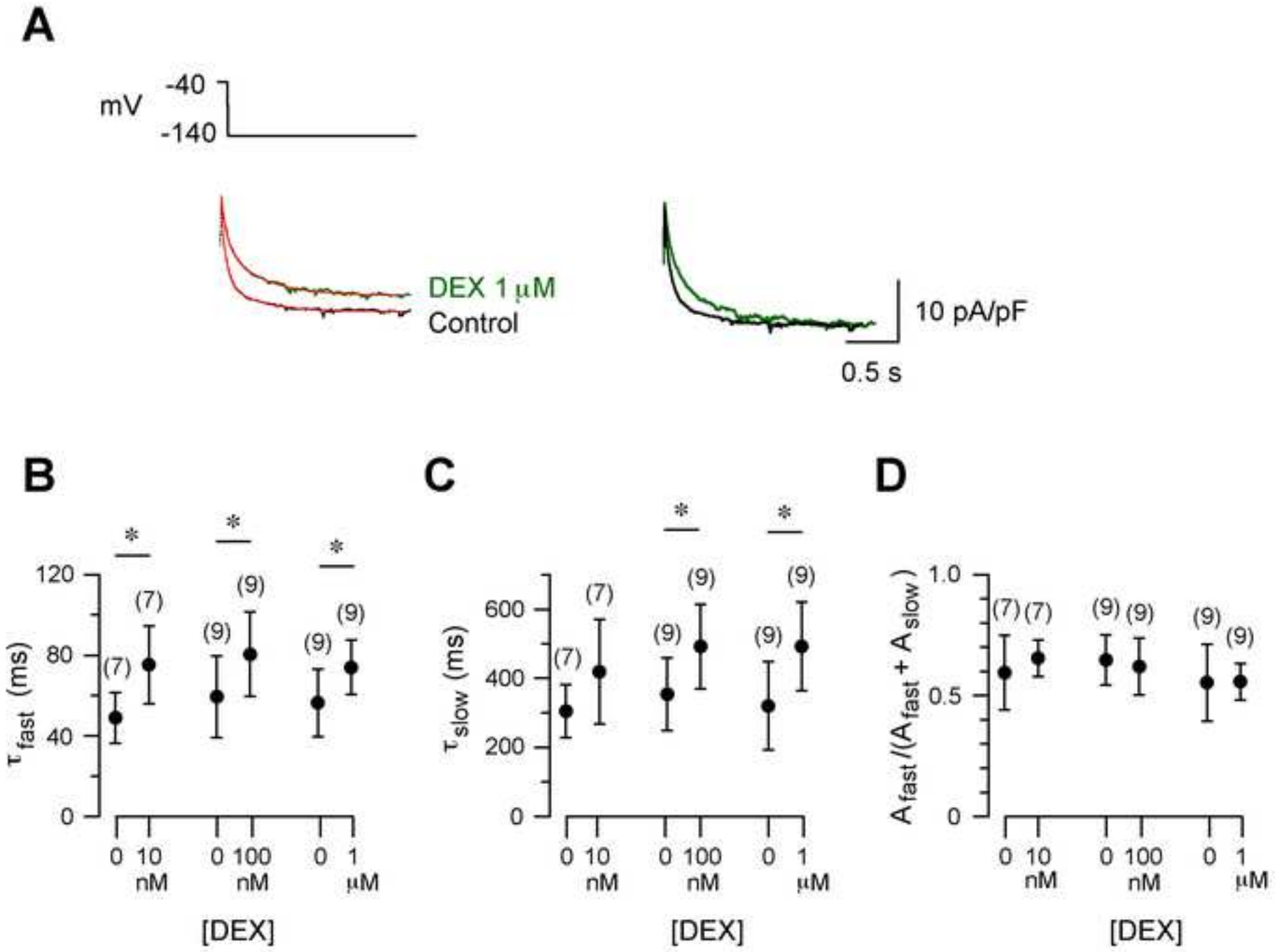

Figure 4

Click here to access/download;Figure;Mariko Ishihara et al-Figure4.tif

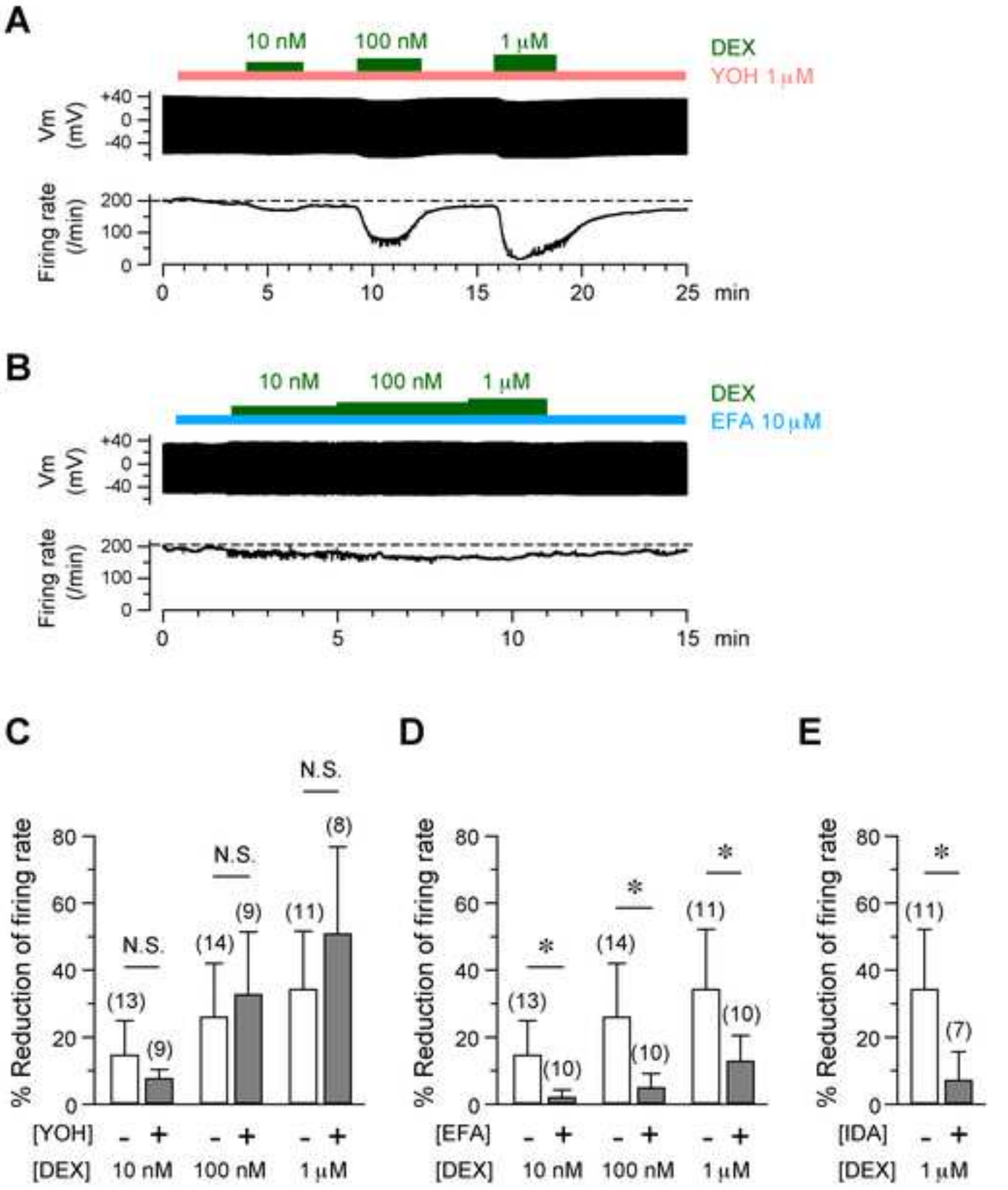

Figure 5

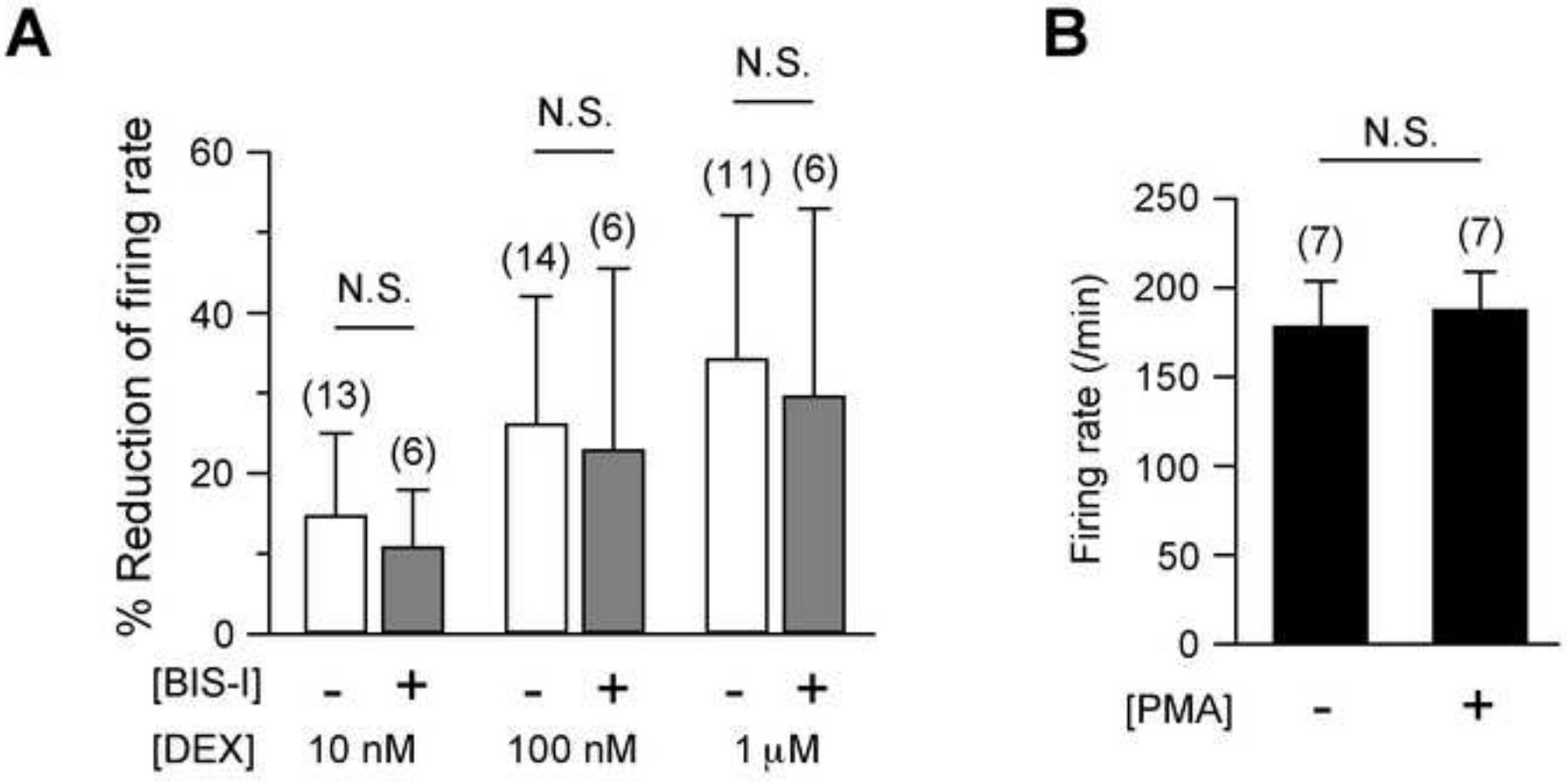

Figure 6

Click here to access/download;Figure;Mariko Ishihara et al-Figure6.tif

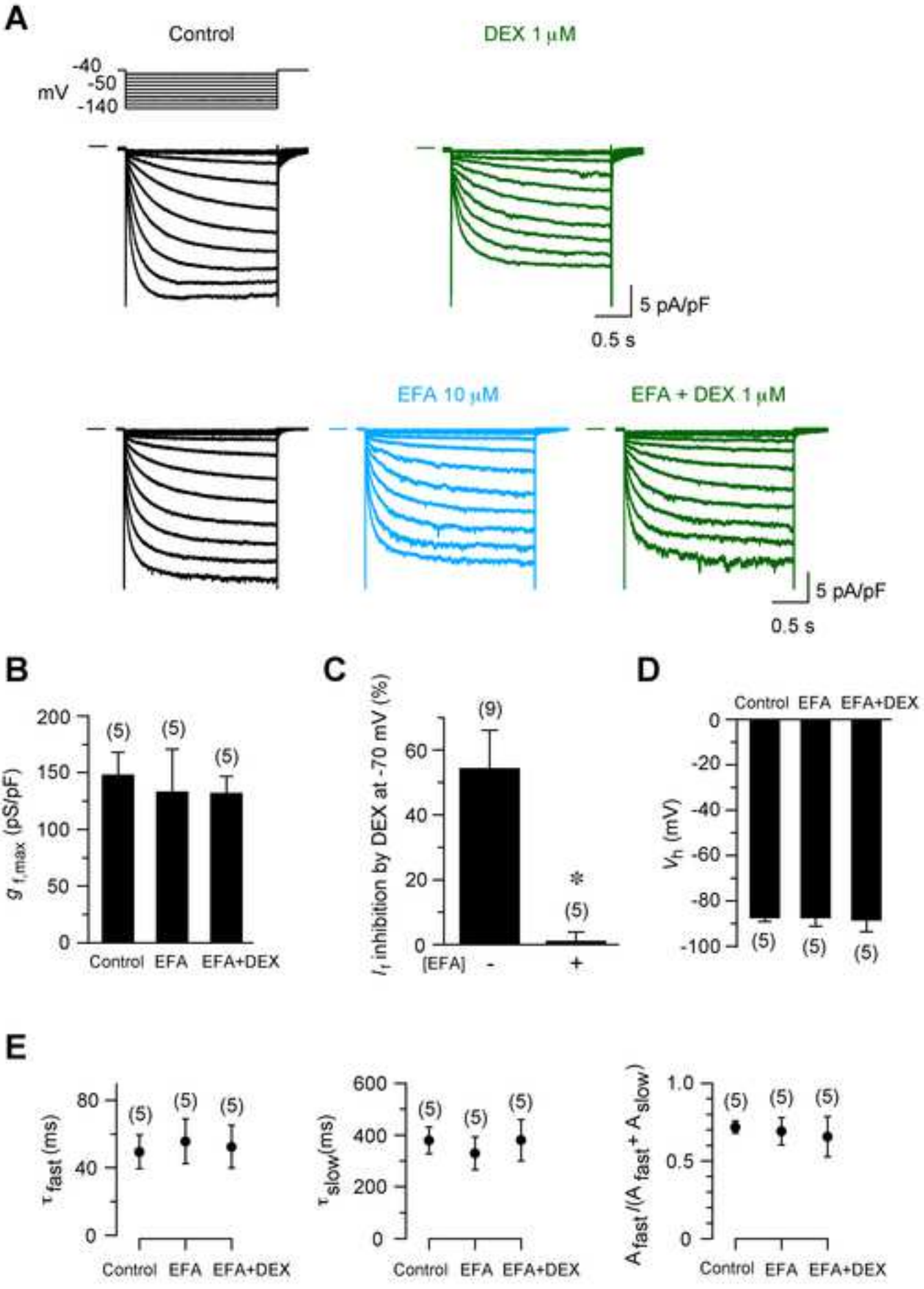

Figure 7

Click here to access/download;Figure;Mariko Ishihara et al-Figure7.tif

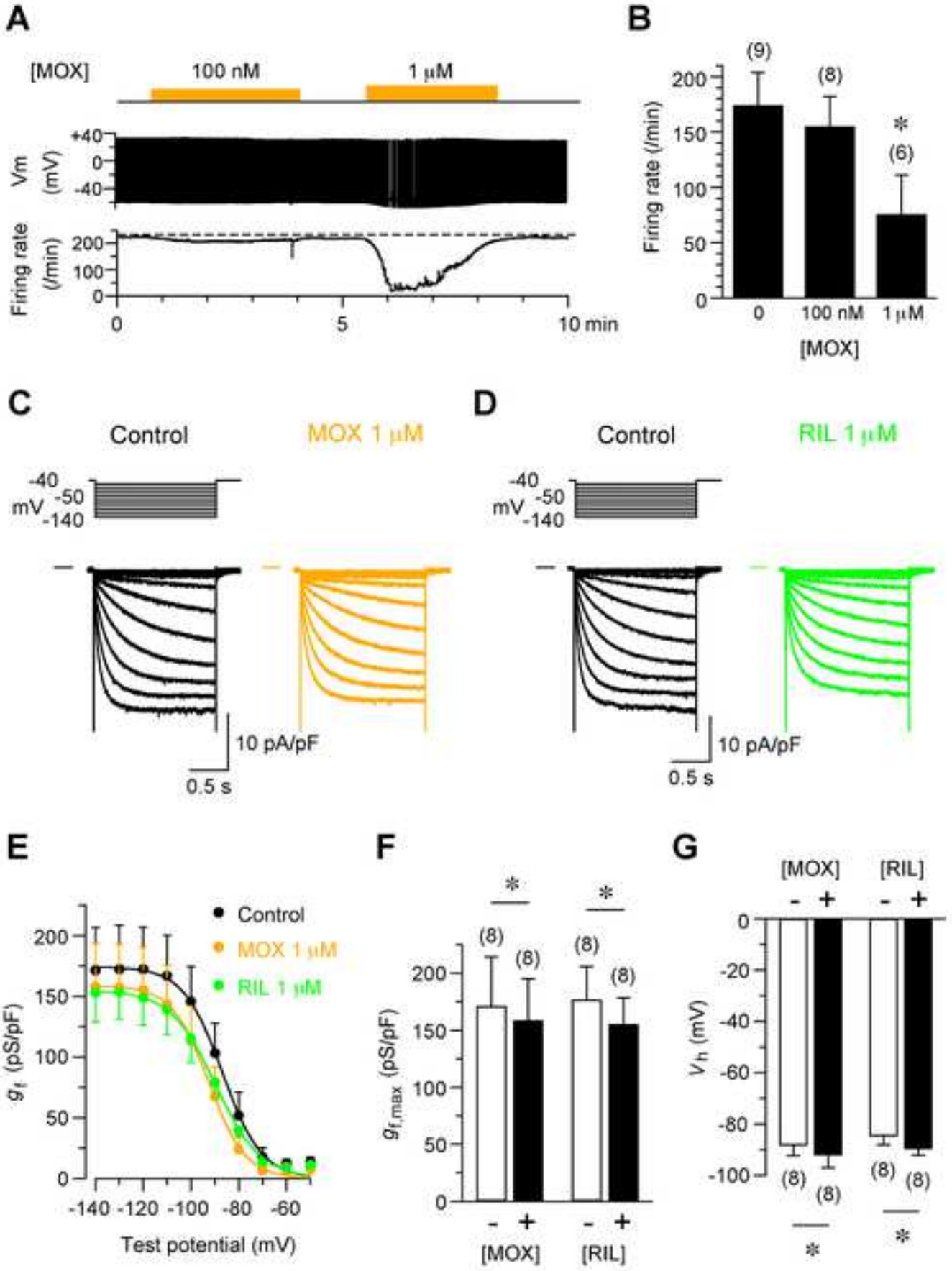

Table 1

Parameters of spontaneous action potentials of SA node cells in the absence and presence of DEX

	Control	**DEX**			
		5 nM	**10 nM**	**100 nM**	**1 μM**
	(n = 18, N = 9)	(n =10, N = 4)	(n = 13, N =7)	(n = 14, N = 8)	(n = 11, N = 6)
APA (mV)	83.5 ± 8.3	84.6 ± 8.4	86.6 ± 7.9	86.3 ± 8.1	86.4 ± 6.2
APD_{50} (ms)	82.5 ± 13.5	92.3 ± 14.9	81.8 ± 16.8	85.5 ± 20.0	81.6 ± 19.9
APD_{90} (ms)	136.4 ± 16.8	145.5 ± 19.0	133.1 ± 23.8	133.3 ± 26.8	133.1 ± 27.2
MDP (mV)	-56.7 ± 6.3	-60.1 ± 7.4	-60.1 ± 6.3	-61.43 ± 6.9	-62.9 ± 6.3
max dV/dt (V/s)	11.7 ± 6.0	10.3 ± 4.3	13.7 ± 7.0	12.9 ± 6.4	13.9 ± 4.6

Data are presented as the mean ± SD and were obtained from the experiments shown in Figure 1. DEX, dexmedetomidine; APA, action potential amplitude; APD_{50}, action potential duration at 50 repolarization; APD_{90}, action potential duration at 90 repolarization; MDP, maximal diastolic potential; max dV/dt, maximal rate of action potential depolarization. These data were analyzed by a one-way ANOVA followed by Dunnett's test.

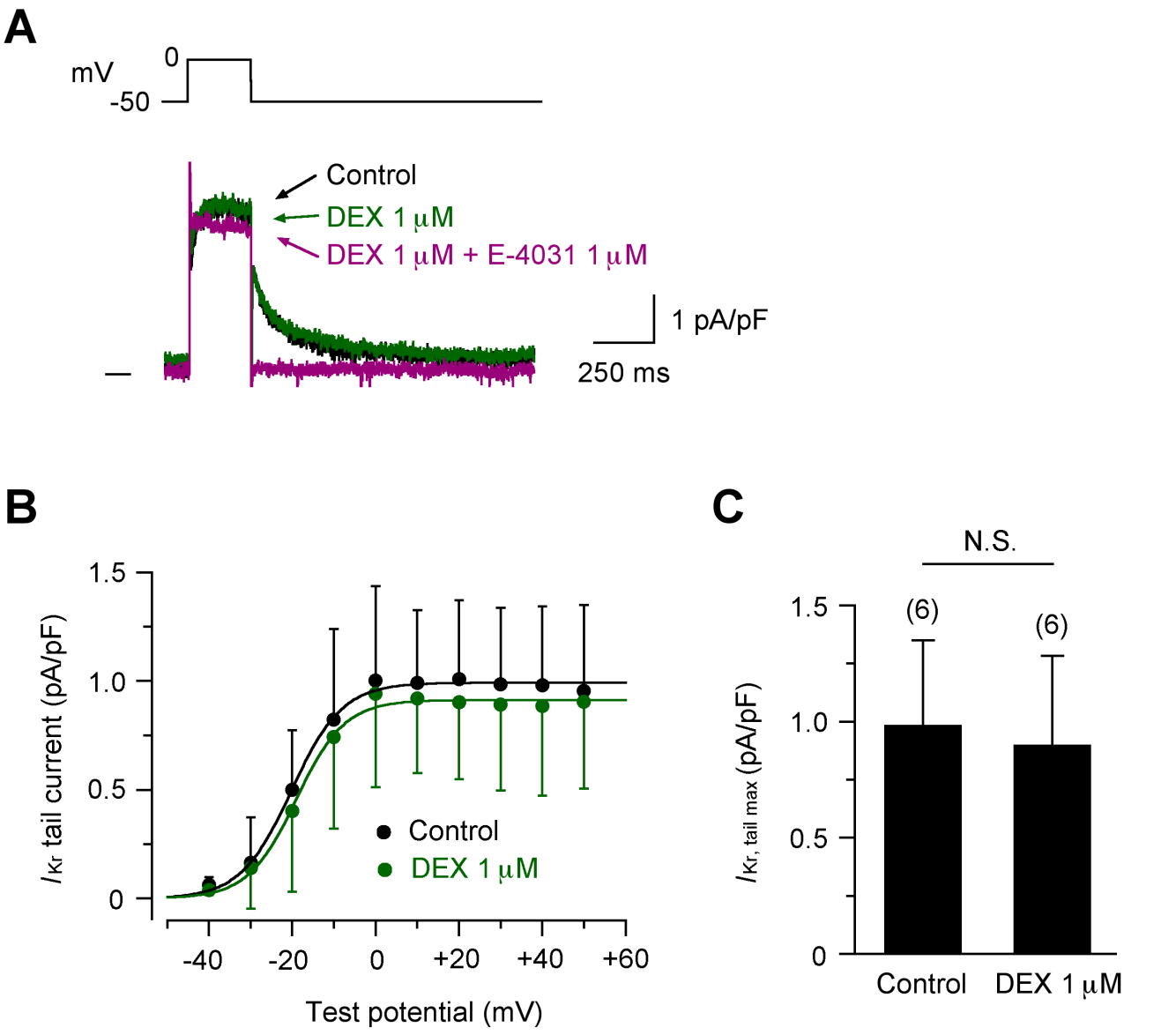

The effect of dexmedetomidine (DEX) on I_{Kr} channel activity. A, Superimposed current traces during 250-ms depolarization steps from a holding potential of -50 mV to test potentials of 0 mV, before (control) and during the administration of DEX (1 μM) for 5 min and 5 min after the subsequent addition of 1 μM E-4031. B, Current-voltage relationships for I_{Kr} tail current, determined as E-4301-sensitive current in the absence (control) and presence of 1 μM DEX. The smooth curves through the data points represent the least-squares fit of the Boltzmann equation ($n = 6$, $N = 4$). C, The maximal amplitude of I_{Kr} ($I_{Kr, tail max}$) in control and in the presence of DEX obtained by Boltzmann fitting ($n = 6$, $N = 4$). The data were analyzed by a paired t test.

Supplemental Figure 1

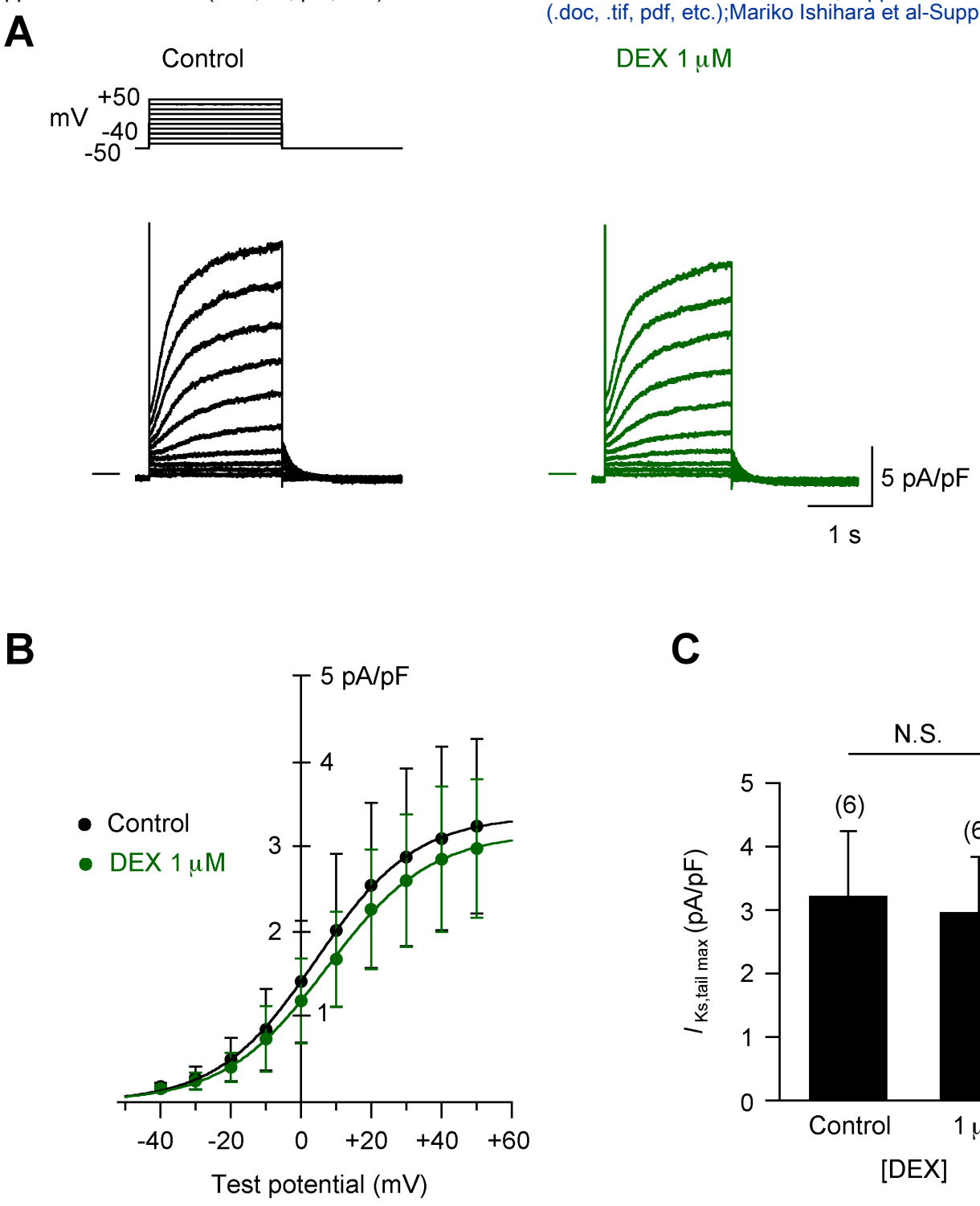

The effect of dexmedetomidine (DEX) on I_{Ks} channel activity. A, Superimposed current traces during 2-s depolarization steps from a holding potential of -50 mV to test potentials of -40 mV to +50 mV, before (control) and during the administration of 1 μM DEX in a cumulative manner for 5 min. B, Current-voltage relationships for I_{Ks} tail currents in the absence and presence of DEX. The smooth curves through the data points represent the least-squares fit of the Boltzmann equation ($n = 6$, $N = 3$). C, The maximal amplitude of I_{Ks} ($I_{Ks,\ tail\ max}$) in the absence (control) and presence of DEX obtained by fitting with the Boltzmann equation($n = 6$, $N = 3$). The data were analyzed by a paired t test.

Supplemental Figure 2

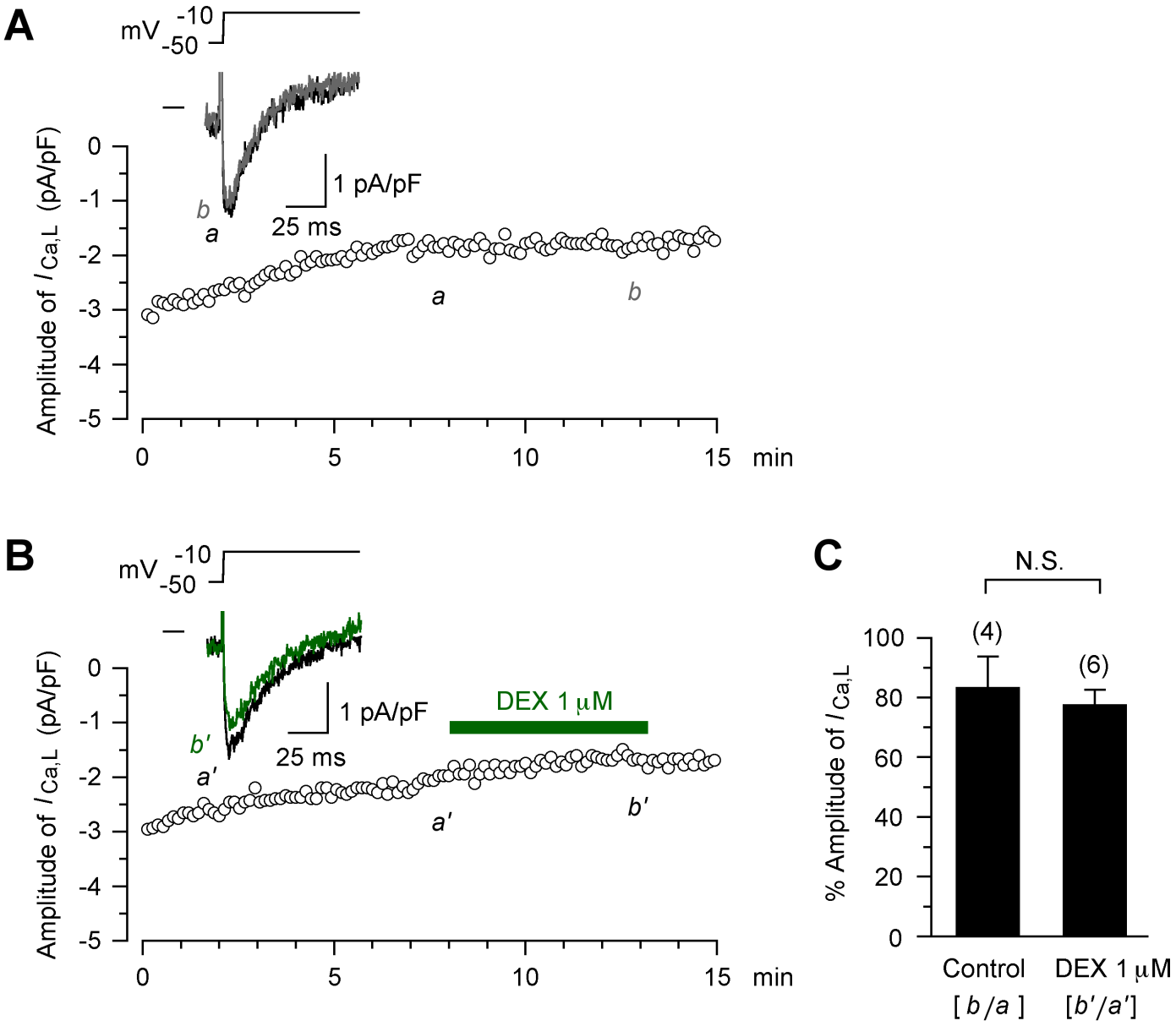

The effect of dexmedetomidine (DEX) on $I_{Ca,L}$ channel activity. A, The time course of the changes in the amplitude of $I_{Ca,L}$ evoked by 500-ms depolarizing steps from a holding potential of -50 mV to test potentials of 0 mV in the absence of DEX for 15 min. B, The time course of the changes in the amplitude of $I_{Ca,L}$ evoked by the same protocol in the presence of 1 μM DEX, 8 min after the start of experiment. C, The percent amplitude of $I_{Ca,L}$ in the absence and presence of DEX at the time points indicated by the characters (a, b in panel A; a', b' in panel B, n = 4-6, N = 3). The data were analyzed by an unpaired t test.

Supplemental Figure 3

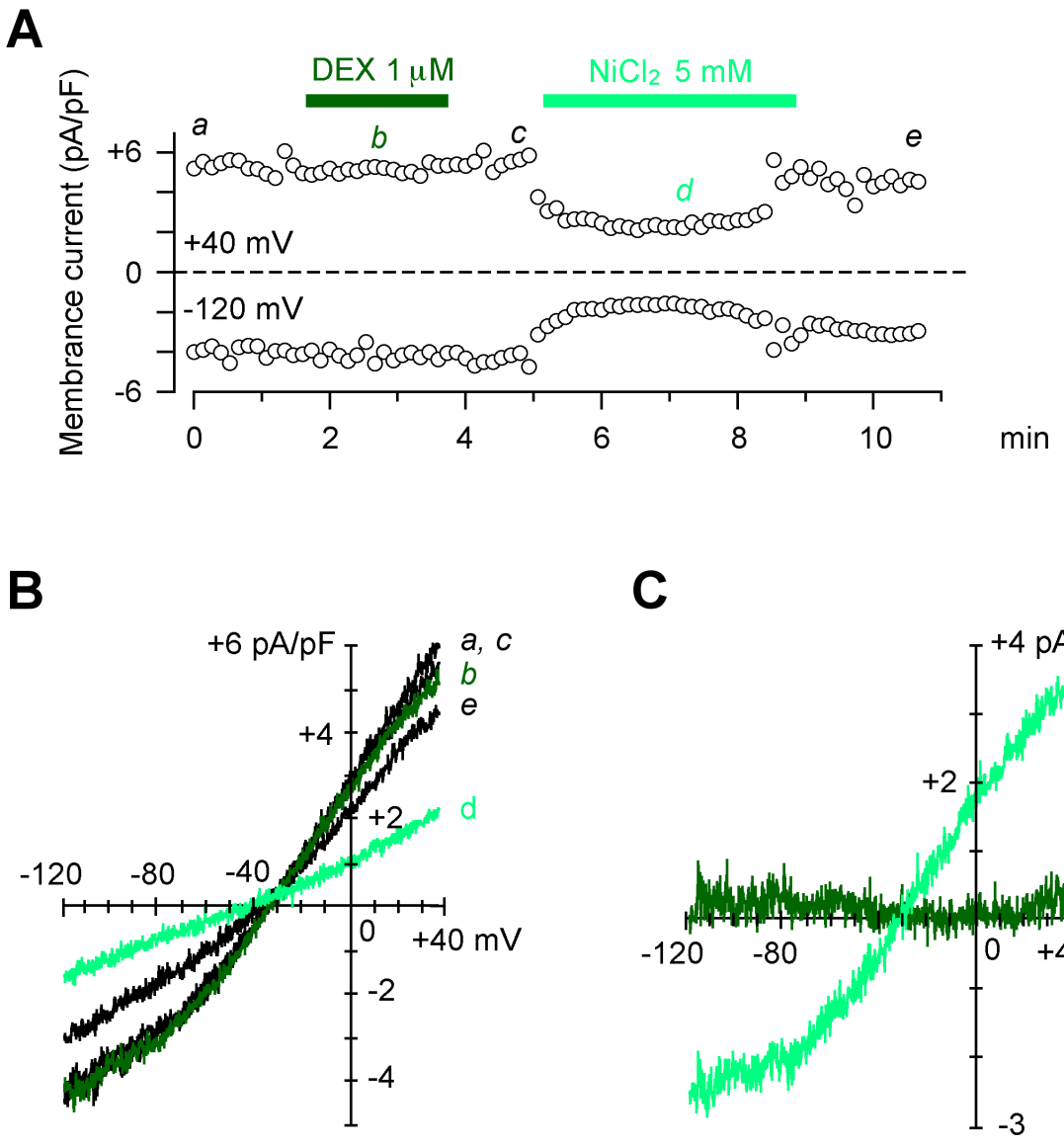

The effect of dexmedetomidine (DEX) on the I_{NCX} activity. (A) The time course of the changes in membrane currents measured at +40 mV and -120 mV in the voltage-ramp protocol, during the administration of 1 μM DEX and 1 mM $NiCl_2$, as indicated. B, The current-voltage relationship of membrane currents at the time points indicated by the characters in panel A. C, The current-voltage relationships for the DEX-sensitive current (a-b) and $NiCl_2$-sensitive current (a-d) obtained by digital subtraction of the current traces shown in panel B ($n = 4$, $N = 2$).

Supplemental Figure 4

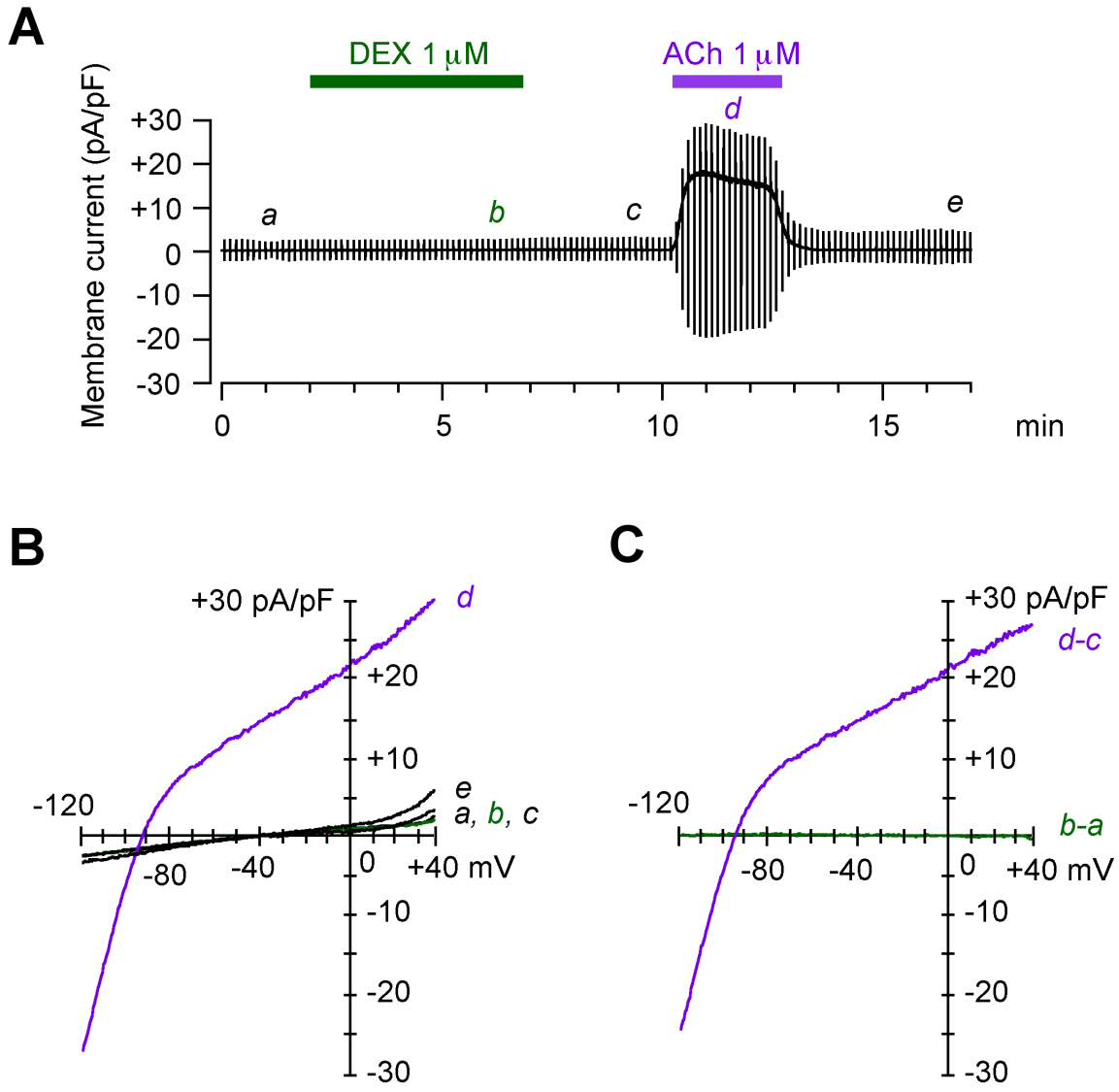

The effect of dexmedetomidine (DEX) on the $I_{K,Ach}$ channel activity. A, The time course of the changes in membrane currents measured at +40 mV and -120 mV in the voltage-ramp protocol, during the administration of 1 μM DEX and 1 μM acetylcholine (ACh). B, The current-voltage relationships for membrane currents recorded at the time points indicated by the characters in panel A. C, The current-voltage relationships for DEX-sensitive current (b-a) and ACh-sensitive current (d-c) obtained by digital subtraction of the current traces shown in panel B ($n = 6$, $N = 3$).

Supplemental Figure 5